X-616-68-370

NASA TM X- 63395

MAGNETIC FIELD EXPERIMENT PIONEERS 6, 7 AND 8

C. S. SCEARCE
C. H. EHRMANN
S. C. CANTARANO
N. F. NESS

SEPTEMBER 1968

GODDARD SPACE FLIGHT CENTER
GREENBELT, MARYLAND

X-616-68-370

MAGNETIC FIELD EXPERIMENT

PIONEERS 6, 7 and 8

C. S. Scearce
C. H. Ehrmann
S. C. Cantarano*
N. F. Ness
Laboratory for Space Sciences
NASA-Goddard Space Flight Center
Greenbelt, Maryland

September 1968

Extraterrestrial Physics Branch Preprint Series

*Now at Marconi Institute of Physics, University of Rome, Roma, Italy

TABLE OF CONTENTS

ABSTRACT

Pioneer 6, 7 and 8 are spin stabilized spacecraft placed in heliocentric orbits in 1965-1967 to study the interplanetary plasma, magnetic field and solar and galactic cosmic rays during the quiet years of the solar cycle, i.e. during the IQSY. The low power, light weight NASA-GSFC magnetic field experiment utilizes a mono-axial fluxgate (saturable inductor) magnetometer. The sensor is mounted on one of three transverse booms 2.1 meters from the spin axis and is perpendicular to the boom axis and at an angle of 54° 45' to the spin axis. Three samples are taken at equal intervals during one spacecraft rotation to yield three independent measurements which are mutually orthogonal and thus define the total vector magnetic field. The magnetometer dynamic range is ±64 gammas (γ) for Pioneer 6 and ±32γ for Pioneer 7 yielding a resolution of ±0.25γ and ±0.125γ respectively. Pioneer 8 incorporates an automatic inflight range switch between two scales of ±32γ, and ±96γ for a resolution of ±0.125γ and ±0.375γ. The accuracy of the experiment is limited by spacecraft associated magnetic fields and the zero drift of the sensor. A nonmagnetic explosive actuated indexing device is used for the first time in satellite experiments to reorient the fluxgate magnetometer by 180° to determine its zero level. The accuracies are estimated to be ±0.25γ, ±0.35γ, and ±0.15γ respectively. A special purpose digital computer was developed to compute time averages when the spacecraft was not transmitting data in real time or was operating at a low bit rate. Successful operation of all experiments has continued since launch to

the date of this final manuscript, October 1968. It should be noted that the design of this experiment was finalized in 1963 and was intended to be a minimum weight and power and ultra low data rate unit.

INTRODUCTION

The Pioneer 6, 7 and 8 are spin stabilized spacecraft launched by the NASA from the Eastern Test Range, Cape Kennedy, Florida on December 16, 1965, August 17, 1966, and December 13, 1967 respectively, into heliocentric orbits. The primary mission of these spacecraft was the study of the interplanetary plasma and magnetic field and solar and galactic cosmic rays. The nominal trajectories of Pioneers 7 and 8 were planned so that the spacecraft would pass close to the sun-earth line at a geocentric distance less than 800 R_E within $\pm 20\, R_E$ of the ecliptic plane to study the extended geomagnetic tail. Orbital parameters are given in Table I.

The Pioneer spacecraft operates in five bit rates, five formats, and four distinct modes for optimum data transmission (see Tables II, II, IV, and V). The bit rates are 512, 256, 64, 16 and 8 bits per second (BPS), and of the five formats three are scientific, one is engineering and both engineering and scientific subcommutator formats. The scientific data frame consists of 32 words, each of which consists of 7 bits: 6 data bits and 1 parity bit. For Pioneers 6 and 7, 512 and 256 BPS are used only with scientific format A while 64, 16 and 8 BPS are used only with scientific format B. Pioneer 8 uses only format B for scientific data transmission. The subcomm consists of 16 and 64 words each for science and engineering and are words 3 and 19 of Formats A, B, C. Thus 16 and 64 scientific frames are required for one complete science and engineering subcomm frame readout respectively.

The scientific data words for the magnetic field experiment are 5, 6, 7 and 8 for format A and 5, 6, 7, 8, 21, 22, 23 and 24 for format B (Table II). The 24 information bits in each word group represent 3 logical 8 bit words of data. Scientific subcomm (format E) words 113 and 114 are used for the status of the experiment and engineering subcomm (format C) word 264 is the temperature of the sensor assembly for Pioneer 6 and 7. Engineering subcomm (format C) word 211 (bits 2, 3, 4, 5, 6) and word 212 (bits 5, 6) are used for the status of the experiment and word 261 for the temperature of the sensor assembly for Pioneer 8. The frame rates are 2.286, 1.143, 0.286, 0.071, 0.036 frames per second for real time transmission.

EXPERIMENT

The magnetic field experiment utilizes a monoaxial fluxgate (saturable inductor) magnetometer. The experiment consists of a sensor assembly and an electronic assembly (Figure 1). The electronic assembly is mounted on the instrument shelf of the spacecraft, which is thermally controlled between 30°F and 90°F. The sensor assembly is mounted on the end of a boom and is enclosed within a canister which provides passive thermal control while the spacecraft is in heliocentric orbit. The electronic assembly consists of four major subassemblies: (a) Time Average Computer (TAC): (b) Analog to Digital Converter (A/D): (c) Power Supply (PS): and (d) Fluxgate Electronics (FG). A block diagram is shown in Figure 2.

The spin stabilized spacecraft permits the use of a unique experiment design in which complete vector measurements of the magnetic field in space are obtained by special orientation of a monoaxial sensor. The axis of the sensor is mounted perpendicular to the boom axis and at an angle of 54° 45' to the spin axis. Three samples at equally spaced intervals during one rotation yield three independent measurements which are mutually orthogonal and thus define the total vector magnetic field.

The telemetry data transmission is not synchronized to the spin of the satellite, so that a complete 3 component measurement is not necessarily read out during each spin period. The experiment will not transfer data to the spacecraft telemetry until all three measurements are completed and stored in the

read out buffer. At the nominal spin rate of 60 RPM, the fastest read out possible is approximately one complete vector measurement every 1.3 seconds. If the experiment has not completed the three samples (X, Y and Z) when telemetry readout is requested, zeros are transmitted. At the faster bit rates of 512 and 256 BPS the experiment is not able to utilize all of the telemetry available.

A spacecraft sun sensor (Figure 2) provides a trigger pulse each rotation and this trigger pulse is used to generate three sample gates equally spaced at 120° intervals during one 360° rotation. The fluxgate analog voltage output is digitized to form an eight (8) bit number (0 to 255). The three orthogonal measurements (24 bits) are stored in data buffer and subsequently transferred to the spacecraft telemetry or if appropriate added to the previous results obtained during the immediately preceding samples.

In this latter mode a time average of the separate orthogonal components is obtained. As the spacecraft recedes from the earth, the telemetry bit rate decreases by a factor of 64, from 512 BPS to 8 BPS. At 512 and 256 BPS only one measurement, three orthogonal components 24 bits, can be transmitted per frame, but the frame rate is faster than sample rate. For 64, 16 and 8 BPS two measurements (48 bits) can be transmitted per frame. At 64 BPS the sampling rate and the telemetry rate are approximately equal. At 16 and 8 BPS there are 7.0 and 14.0 seconds between each telemetry readout. In addition, at certain intervals in the operation of the spacecraft, non real time transmission of data takes place so that the spacecraft on-board memory system stores

discrete samples of data at time intervals long compared to the spin period. This mode of operation is referred to as Duty Cycle Storage (DCS) mode. The time intervals between the stored frames for the different DCS modes are 2 min. 8 sec., 4 min. 16 sec., 8 min. 32 sec. and 17 min. 4 sec., (Table VIII).

For unique analysis of the experiment data it is necessary to provide a means of adapting the experiment to these varying telemetry data rates. To accomplish this the magnetic field experiment includes a Time Average Computer (TAC). When the telemetry bit rate is 16 BPS or lower (and also during DCS) the time average computer is utilized. The experiment computer will add the incoming data sample (X, Y, or Z) to the appropriate preceding stored data (X, Y, or Z) and then store the new sum in the buffer. After the appropriate number of samples have been made the computer will divide the sum by the number of samples added, which is 2^2, 2^3, 2^6, 2^7, 2^8 samples. In the time average mode each component (X, Y, and Z) is sampled each revolution. At the nominal spin rate of 60 RPM the computing time for the different modes are: 4 sec, 8 sec, 1 min. 4 sec., 2 min. 8 sec. and 4 min. 16 sec., respectively. As seen from the sampling time the experiment will average the data for about 50% of the time between readouts (Table VII).

ACCURACY

Magnetic Noise

One of the limiting factors in measuring the magnetic field in space is the relative contribution of the magnetic field associated with the spacecraft. The sensor is mounted on one of three booms approximately 2.1 meters from the center or spin axis. Detailed test mapping has indicated that the interference from Pioneer 6, 7 and 8 was less than 0.125, 0.35 and 0.2γ respectively, (TRW Systems, Table VIII).

Zero Level Drift

A major limitation of the fluxgate magnetometer accuracy is the possibility of undetected zero level drifts. A device for establishing the accuracy of the fluxgate magnetometer in flight was developed and successfully operated for the first time in a space experiment. This calibration is accomplished by physically reversing the direction of the sensor by 180° on the end of the boom. The device itself consists of a small lightweight spring energized clock escapement mechanism which is activated by ground command. The zero calibration in flight was made to within $\pm 0.25\gamma$. A sample of the results obtained from Pioneer 6 is shown in Figure 3 (Ness et al., 1966). The post flight zero calibrations are shown in Table IX.

Calibration, Post Flight:

Sensitivity calibration is accomplished by the addition of a known and accurately calibrated external magnetic field to the sensor and measuring the

subsequent change in the digitized representation. Approximately once per day the sensitivity calibration of the magnetometer is exercised and compared to the pre-flight sensitivity calibration (Figure 4). The uniform scatter about the pre-flight value independent of the ambient average value checks the pre-flight linearity of the instrument.

Calibration, Pre-Flight:

The experiment is calibrated in the GSFC T&E 20 foot coil facilities before and after the environmental acceptance tests. The environmental acceptance tests are performed at GSFC before the experiment is delivered to the Pioneer Project to be integrated into the Pioneer Spacecraft. The experiment is calibrated at the Malibu Coil System with the spacecraft in free flight configuration, excepting for the use of an external power supply, for pre and post spacecraft environmental acceptance tests. There are some differences noted between the final calibration at GSFC and the final calibration at Malibu (Table X and XI and Figure 5). The difference is probably contributed by the difference in the impedance of the boom cable and the test cable used at GSFC. At Malibu all modes of operation of the spacecraft and experiments were checked to insure there was no interference either from the subsystems of the experiments.

EXPLOSIVE ACTUATED INDEXING DEVICE

The nonmagnetic, explosive actuated indexing device (Baurnschub, 1966) is a mechanism to reorient the fluxgate magnetometer in space flight (Figure 6).

The magnetometer sensor and a coil of tape cable are positioned upon a rotatable shaft. Attached to this shaft is one end of a power spring; the opposite end of this spring is attached to the spring housing, which in turn fastens to the actuator housing. These housings are concentric to the shaft so that when the spring is wound, a torque develops which will rotate the shaft and housings in opposite directions.

The escapement which controls this rotation consists of a ratchet, which is attached to the shaft, and a mating part designated as sensor ratchet arm. The 180 degree indexing of the magnetometer sensor is a function of the shape and pivoting of this arm. A stable state is maintained by an off-center spring fastened from the arm to the main structure across the pivot point. A second arm is attached to the previously mentioned arm and pivots with it. The arm engages the piston actuator housing and alternately mates the opposite impact surfaces with a pair of explosive piston actuators. Eleven pairs of piston actuators are housed about the periphery of this disk. Two actuators are used for redundancy. Figure 7 shows both piston actuators that have been fired and those that will move into position. The housing is indexed by means of protruding pins that engage the ratchet arm. The spring housing also engages four of these pins to transmit the drive torque.

The force detonation extends the piston 1/8 inch. The piston is directed against one of the piston impact surfaces of the second ratchet arm. The ratchet arm pivots outwardly and carries the first ratchet arm along with it. The ratchet, along with the main shaft and sensor, disengages the first ratchet arm and rotates 180°. It then engages the opposite side of the ratchet arm, coming to rest in its other position.

Simultaneously, the second ratchet arm permits the piston actuator housing to rotate 15 degrees. In this manner, another pair of piston actuators are positioned under the opposite piston surface and are available for another reorientation command. Figure 8 shows the ratchet arms, and illustrates the piston impact surfaces, the stop for the 180° ratchet, and the stops for the piston actuator housing. Figure 9 illustrates the piston actuator housing and the 11 ratchet pins that engage the second ratchet arm. A printed circuit commutator is attached to the other side and the piston actuator leads are soldered to terminals on the commutator. This assembly rotates on the main shaft, but in the direction opposite to that of the magnetometer.

In Figure 10 the ratchet and spring are shown attached to the main shaft. The hole at the far end is the magnetometer pinhole, and the protruding pin at the near end operates a pair of switches that indicate the magnetometer position.

FLUXGATE MAGNETOMETER

The fluxgate magnetometer is a single component Heliflux magnetometer developed and manufactured by the Schonstedt Instrument Company (Figure 11). The instrument consists of a magnetic field sensor and an electronics unit. The specifications are shown in Tables X and XI and Figure 5.

The fluxgate principle, which has been applied to devices of widely varying configuration, has been explained and analyzed in a number of publications: Alldredge (1955), Geyger (1960), Gozor (1951), Hughes & Sons (1947), Palmer (1953) and Schonstedt (1961). All fluxgate magnetometers have in common the use of a ferromagnetic core (or cores) which is excited by a driving, or gating, magnetic field generated by current in a coil which contains the core. The flux induced in the core by the gating field is modified by an external magnetic field which generates even harmonics on the output winding. The gating field's effect upon the core may be considered as permeability modulation.

Modulation of the core material's permeability in turn modulates the flux θ_x, which is coupled into the core from the field being sensed, H_x. The exact manner in which the permeability of the core varies as a function of gating field depends upon the principal factors:

1. The basic configuration chosen, eg., either a parallel or an orthogonally gated core or any other special configuration.
2. The type of core material used and its magnetic history.
3. The wave shape of the gating field.

4. The geometry of the core.

Figure 12 illustrates the process whereby a gating field H_g, applied to a core in the presence of an external field, H_x, provides an output proportional to H_x. This figure shows how the fluxgate process results in an output consisting of even harmonics of the gating frequency. In addition to the ideal output described above, the output of a fluxgate magnetometer usually contains these undesired components:

1. Signal due to coupling between the gating field and the output.
2. Signal generated as a result of anisotropies and inhomogenetics in the magnetometer core.
3. Noise from sources such as Barkhausen noise, coupled noise and structural noise.
4. Signal generated by remanent core magnetization.

The Heliflux sensor is a cross between parallel and orthogonally gated cores (Figure 13). Two strips of core material are wound in a pair of helices in opposite directions on a hollow ceramic tube and the ends are mechanically connected. The primary winding is wound as a toroid on the ceramic tube. When the AC current is applied to the primary winding, the magnetizing field has components both parallel and transverse to the core strips. The entire core is cyclically saturated in the X direction by the gating field to minimize the remanent magnetization, or core memory. The secondary winding is wound around the core, perpendicular to the primary winding. The coupling between

the gating field and the core output is dependent upon the physical orientation of the gating and output windings. See (Schonstedt, 1961) for detailed construction.

The electronics unit is comprised of an oscillator and driver, preamplifier and amplifier, phase detector, rectifier, and voltage bias (Figure 14). The oscillator produces an AC signal of ~12 kHz which is power amplified by TR 102 and TR 103 and fed through the primary winding of the sensor to cylically drive the magnetic core of the sensor into saturation through T 102. The frequency and amplitude of the driver is temperature compensated by D 101, D 102, and D 103. The presence of a magnetic field along the axis of the sensor results in the generation of a second-harmonic voltage in the secondary winding of the sensor. The amplitude of the second-harmonic voltage is proportional to the magnitude of the magnetic field and the phase dependent upon the direction of the magnetic field, the phase changing by 180° if the field direction is reversed.

The second-harmonic signal is amplified by the tuned preamplifier and amplifier and fed to the phase detector by T 301. The second-harmonic signal is compared to the phase of the reference signal. The driving signal frequency is doubled through T 103 and fed to the phase detector T 301 as the reference signal. The second-harmonic signal is superimposed on the reference voltage in such a manner that one peak of the reference voltage is increased and the other peak is decreased. This modification of the reference voltage causes C 307 and C 308 to be charged unequally, thereby creating a voltage differential across the output of the rectifier. Resistors R 307 and R 308 connected across

C 307 and C 308 provide leakage paths for discharging the capacitors. Capacitor C 306 is used to reduce the AC ripple and determines the frequency response of the output.

Resistors R 310, R 312, and R 313 are series connected across the supply voltage. One leg of the rectifier circuit is connected to the common junction of R 310 and R 312 to bias this leg at a nominal 2.5 VDC. For a condition of zero magnetic field along the sensor's axis the output signal will be at the nominal 2.5 volt bias level. For other field conditions, the output signal will be less than or greater than the bias level depending upon the direction of the magnetic field with respect to the sensor axis.

POWER SUPPLY MODULE

The power supply module contains the experiment power converter, which supplies +6 volts for logic and ± 12 volts and a precision +5 volt reference for the ADC and the fluxgate.

The housekeeping Data System (Figure 15) monitors the operating mode of the TAC, the position of the flipper, the state of the fluxgate calibrator, the receipt of a flip command and the condition of the timing generator. It consists of a 3 bit programming counter with control circuitry of two diode decoding matrices and an output driver.

The operation is as follows: spacecraft shift pulses are gated with 1) subcommutator word gate 13 in gate A, 2) word gate 14 in gate B and 3) the complement of the 000 state of the three counter stages in gate C. These three functions are "or" ed in D and fed as input to the first counter stage.

If either Wd 13 or Wd 14 becomes true, shift pulses are then fed to the counter which counts up from the 000 state. After 6 shift pulses the word gate again goes false leaving the counter in the 110 state. Gate E however is now true allowing pulses through C until the 000 state is reached once more.

The first six states of the counter are decoded and "and" ed with the input data by two diode resistor gate matrices whose outputs are "or" ed in two diode resistor gates, which are clamped false except when subcomm word gates are present. The outputs from these gates are then "or" ed and shaped for output to the spacecraft.

EXPLOSIVE ACTUATION AND CALIBRATION

The fluxgate calibrator receives an impulse command from the spacecraft, which is stored in a binary until a subcomm wd 13 occurs. The leading edge of this word is "and" ed with the stored command and thereby turns on a second binary which controls a transistor switch to feed current to the fluxgate calibration coil. The next subcomm wd 14 shuts off the command storage binary and the leading edge of the subsequent subcomm wd 13 shuts off the calibration current. The state of the current control binary is fed to the housekeeping data system for monitoring when the experiment is in the calibrate mode.

The ordnance circuit (Figure 16) accepts an impulse command from the spacecraft and uses it to set a binary (A) whose output is used to charge a large capacitor (C1). When this capacitor is charged to the threshold voltage of a unijunction transistor (Q1) whose gate is connected to the positive terminal of the capacitor, the transistor fires, in turn triggering an SCR (Q2) which discharges the capacitor through the explosive actuators in the fluxgate flipper, rotating it 180°. The SCR firing is detected by a transistor (Q3) which resets the binary turning off the charging current to the capacitors. To prevent the circuit from firing when power is turned on, the network (R_1, C_2) holds the collector Q3 negative for a short period, holding the binary reset. A second binary (B) is triggered by the command. Its output goes to the housekeeping data system. A change of state of this binary confirms receipt of the flip command.

In addition this module contains the two counters used to monitor the TAC operating mode and the condition of the timing generator. The first of these counters, which is four bits in length, counts the number of times the accumulated field samples stored in the TAC are divided by two before transmission. This number indicates the actual operating mode of the TAC. The second counter monitors the number of clock pulses by which the timing generator is in error each spin period. The outputs of both these counters are telemetered via the experiment sub commutator.

TIMING AND ADC MODULE

The Timing and ADC module contains the main timing generator, analog to digital converter and the buffer register. The timing generator, shown in Figure 17 provides all control pulses for data sampling and consists of a voltage controlled oscillator (VCO) which is constrained by a digital feedback scheme to operate at a fixed number of cycles per spin period, a main counter from which the feedback scheme for the oscillator is derived and a group of gates which decode the status of the main counter to generate the required timing pulses for the rest of the experiment.

An operational amplifier integrator is used as a storage element to hold a control voltage for the VCO. The stored voltage may be modified by making true the input of one of two current gating circuits, one to raise the voltage, one to lower it.

The occurrence of every sun pulse (once per spacecraft spin) phase synchronizes the VCO to eliminate least count error, and resets the main counter. The output of the VCO is then counted in the main counter until one of two conditions occurs, either 1536 counts are accumulated or another sun pulse is sensed. In the first case the VCO frequency is too high, so the counter is inhibited and a down frequency correction is applied to the holding circuitry until the next sun pulse.

If a see-sun pulse is sensed before the counter is filled, the VCO frequency is too low and must be raised.

This is accomplished with an auxiliary correction counter, which operates in one of two modes, to time an up-frequency correction interval. If the count is low by more than 32 a gate (G) "and" ing the six most significant bits of the counter is false at the see-sun pulse time. Its complement ($\bar{G}$) is "and" ed with the sun pulse and fed as input to the error counter, which is in the 00000 state due to gates B, C and D which allow VCO pulses to be counted if it is in any other state. This sun pulse takes the counter out of its inhibited state and allows it to complete one full count sequence. $\bar{D}$, which is true during the time the error counter is running, is fed to the up-correction current driver raising the holding circuit voltage.

In the case of an error of less and 32 counts gate G becomes true and, at sun pulse time, the states of the least significant 5 bits of the main counter are transferred to the error counter removing it from its inhibited state. It then receives counts through gates B, C and D until it refills. This number of counts is equal to the main counter error count, allowing a correction to be applied for a shorter and shorter period of time as the proper VCO frequency is reached.

The dual up-frequency correction is chosen primarily to minimize the number of circuits required. In principle an error counter, eleven bits in length, operating in the second mode described is sufficient to do the job, but errors of this magnitude are very improbable, so a shorter error counter is used.

This is no longer sufficient, however, since if the count error is a multiple of 32 (2^5) counts 00000, would be transferred to the error counter and be

recognized as no count error. To circumvent this difficulty large errors are detected by gate G and a full 32 count correction interval is applied.

The number 1536 is chosen as the reference count because it gives resolution of greater than ± 1/8 degree (The limit of sampling accuracy) it is divisible by 3 (the number of samples per spin) and this quotient is a binary multiple = 512 (simplifying the design of the counter).

Derived from the main counter are a group of sampling control signals

a) An X, Y and Z gate, each 512 counts long and occurring sequentially to define the three field sampling intervals. These are decoded from the states of the two most significant bits of the main counter.

b) Six control signals for the analog to digital converter which are derived from the states of the three least significant bits of the counter.

c) A sample gate which occurs at sun pulse time and at the first VCO pulse of the X and Z gate, and commands the ADC to take a field sample.

d) A transfer pulse on the ninth clock pulse after the sample gate which transfers the converted sample to the output shift register.

e) A group of 16 shift pulses beginning with the 17th and ending with the 32nd VCO pulse after each sample gate, which are used to shift data into and to operate the Time Average Computer.

ANALOG TO DIGITAL CONVERTER

The analog to digital converter used in Figure 18 is of the successive approximation, weighted resistor network type. It is eight bits in length, and maintains an accuracy and integral linearity of better than $\pm 1/2$ bit over the entire range of operating conditions.

The logical portion of the ADC consists of 8 decoding gates, 8 storage binaries, one inhibit binary, and some additional control gating. The linear portion consists of an 8 bit weighted resistor network and its control switches, an operational amplifier current-to-voltage converter and a voltage comparator.

The weighted resistor network consists of eight chains of resistors, having binary multiple values from 20K through 2400K ohms, with one end of each tied to the +5 volt reference, the other ends tied together and with center taps tied through transistor switches (operated in the inverted mode) to ground. By turning any of these switches off or on, it is possible to feed a current of fixed value to the summing point or to clamp that current off. One of several schemes may be used to accomplish this current switching (Figure 19). In circuit A, base drive current is drawn from the reference supply, and since for minimum offset error in the on state it is desirable to operate the switch in the inverted mode, this current may be of the order of 0.5 to 1 ma per switch requiring a reference supply with good load regulation, and an additional high voltage supply to bias the switches off.

Circuit G uses FET switch which introduces no load to the reference supply. However for effective operation a large positive voltage is required to turn the switch off, and FET's with on resistances low with respect to the weighting resistor were unavailable at the time the experiment was designed.

Circuit B overcomes these problems in that control current is supplied to ground easing the load regulation requirements for the reference supply, since the load current changes only by a factor of two for any combination of switch states, with center tapped resistors. It may be shown that offset error is minimum if the tape point is chosen at the mid point of the resistor. In addition this circuit may be operated directly from the logic level voltages and a switching transistor with suitably low offset voltage (1 mv at 0.5 ma) was readily available.

The common point of the network is tied to the summing junction of an operational amplifier (with a 10K feedback resistor), which acts as a current to voltage converter.

It may be seen that by turning on all possible combinations of the 8 switches any increment of voltage between zero and full scale may be generated at the output. This voltage is compared to the magnetometer output in a voltage comparison circuit consisting of the differential front end of the operational amplifier followed by a Schmidt trigger to convert to logic levels. The output of the comparator is used as feedback to control the operation of the ADC.

The converter operates as follows:

On the occurrence of a sample gate the first (128) storage binary is set to one and all other binaries including the inhibit binary are set to zero. This causes the 128 current to be gated on, comparing the input voltage with half scale. If it is less than half scale the output of the comparator becomes true.

The first clock pulse following the sample gate is decoded by gate A and used to set the 64 binary and to reset the 128 binary via gates I and Q if the comparator is true, leaving the comparison voltage at 1/4 or 3/4. The second clock pulse decoded by B sets the 32 binary and resets via J and R the 64 on condition of the voltage comparator. This action continues for 5 more clock pulses. The eighth pulse is used to reset the 1 binary on condition of the comparator and to set the inhibit binary disabling the converter until the next sample gate. The storage binaries now hold a binary number representing the magnetometer output voltage.

The "1" outputs of these binaries are loaded via a set of transfer gates into a shift register at transfer pulse time for transmission to the TAC.

TIME AVERAGE COMPUTER

The Time Average Computer (TAC) performs separate averages of the three orthogonal components of the magnetic field over a variable number of spacecraft revolutions, the number of data points selected depending upon the mode of the telemetry system. The averaging process results in smoothing out the fluctuations yielding a physically more significant parameter, the average steady state value of the field, rather than a single value every readout. The computer is hardwire programmed and the number of data points in an average is a function of the telemetry mode. For simplicity the averaging is accomplished by shifting the binary point rather than arithmetical division. Thus the number of data points in an average is the highest integer power of 2 which is lower than the computed number of data points possible between telemetry readout. The number of data points possible between telemetry readout is determined by computing the number of revolutions between telemetry readout for a spin rate of 60 ± 10 RPM.

Table VII gives the number of data points in the average for real time transmission and DCS mode; for example in real time at 8 bps, 14 data points could be accumulated but the average is computed over only 2^3 or (8) data points and the division is implemented by shifting the binary point 3 places in the accumulator register.

Figure 20 is a block diagram of the time average unit. The X, Y and Z accumulator registers (initially cleared) are loaded with the corresponding

component measurements appearing at DATA and coming from the 8 bit ADC (least significant bit first) via the serial adder; the ADD pulses accompanying the DATA are addressed to the proper register shift line.

Each measurement is added to the contents of the corresponding register, selected by the input gates. The process continues for 2^i data points, so that at the end of this accumulation phase the three registers will contain the measurements.

$$\sum_{k=1}^{2^i} X_k \qquad \sum_{k=1}^{2^i} Y_k \qquad \sum_{k=1}^{2^i} Z_k$$

Then the content of the registers are shifted by i positions, which corresponds to a divide by 2^i, with the average values contained in the last 8 bit portion of each register.

During these two cycles of operation, the gating networks G1, G2 and G3 gate the data through the register. The average values are ready to be transferred to the telemetry: the first incoming sync word will address the bit sync pulses into the shift lines, the three 8 bit sections of the registers containing the information are connected in series via G2 and G3 to permit the readout of the three components. After the telemetry readout the registers are cleared by setting the first stage of the X register to "1," which was cleared by the readout.

Data input to the three registers are inhibited during readout. Clear pulses are addressed to all three shift lines until this "1" in X_0 reaches the "clear control" flip flop, then the clear pulses are interrupted. The operational cycle

is conditioned by the control logic: the sample time occurs three times per spin period and the register's cleared signal sets the accumulation control flip flop initiating the accumulation cycle. The 9 bit counter counts the number of data points being accumulated and, when the programmed 2^i points is reached, an "end average" pulse is furnished by the detection gates. The "end average" pulse resets the accumulation control flip flop and commands the shift i generator. After the shifting is completed the readout logic is enabled.

After telemetry readout the X_0 flip flop is set to "1" and the clear operation takes place. The "registers cleared signal" begins a new cycle. The accumulation begins with the first incoming component measurement which is addressed to the proper register, independently of whether it is an X, Y, or Z component. The accumulation is completed when the proper number of samples is accumulated in each of the three registers. In real time, when the averaging process is not used, a set (X, Y, Z) or (Y, Z, X) sequentially in time will be loaded to the proper register, depending on whether the first incoming component is an X, Y, or Z. One spin period T_s is thus sufficient to complete a set of three components.

In the DCS mode the average values computed during the coast time are readout twice per frame for redundancy, in this mode the data is recirculated in the last 8 bit positions of the registers via gates G1, G2 and G3 during the telemetry readout of words 5, 6, 7 and 8. Figure 21 is the logic diagram of the

serial adder; the four NOR gates 1 to 4 and inverter 5 perform the gating function $B = X_A X_G + Y_A Y_G + Z_A Z_G$ thus entering into the adder

$$X_A \text{ if } X_G = 1,\ Y_A \text{ if } Y_G = 1 \text{ and } Z_A \text{ if } Z_G = 1$$

It is assumed in the following that when $X_G = 1$, X_A is entering into the adder and the incoming DATA X_i is a new sample of the X component.

The logic function of gates 5 and 6 is the coincidence $X_i \odot X_A \equiv X_i X_A + \bar{X}_i \bar{X}_A$; therefore the output of the adder is:

$$\text{SUM} = X_i \odot X_A \odot C_i = X_i \oplus X_A \oplus C_i$$

where $\oplus$ is for the ex-OR function.

The above expression for SUM can be demonstrated by applying the following relations

$$X_i \odot X_A = \overline{X_i \oplus X_A} = \bar{A}$$

and

$$\bar{A} \odot C_i = A \oplus C_i$$

The carry is

$$C_{i+1} = X_i X_A C_i + X_A \bar{C}_i + \bar{X}_i X_A C_i + X_i X_A C_i = (X_i \oplus X_A) C_i + X_i X_A$$

and is implemented with NOR gates 8, 9 and 10 and inverted 11. The carry $C_{i+1}^{(1)}$ is transferred into the memory flip flop F1 to be presented to the adder

with the next incoming higher order bit. Figure 22 shows the accumulator registers and associated gating network of the shift pulses for the shift lines. The last flip flop of the X register is the "clear control" FF and its output X18 is the "registers cleared" signal.

Note (1) $\overline{\overline{X_i \odot X_A} + \overline{C}_i + \overline{X}_i + \overline{X}_A} = \overline{\overline{X_i \oplus X_A} + \overline{C}_i + X_i X_A} = (\overline{X_i \oplus X_A})C_i + X_i X_A = \overline{C}_{i+1}$

The data is transferred to the telemetry data system via the output buffer during the readout cycle. Figure 23 shows the network determining the number of samples in the average as a function of the telemetry mode. Gates 3, 4, 5 and 6 determine the number of samples in DCS mode and gates 8, 9 and 10 determine the number of samples in real time transmissions. Only one of the $\overline{M}_i$ output lines will be at the logical "zero" (The subscript "i" indicating that 2^i samples will be accumulated). The output $\overline{M}_0$ is derived by a NAND of all the other outputs, so that it will be "zero" when all the other $\overline{M}_i$ lines are at "1," for failsafe operation.

Figure 24 is the complete logic diagram of the programmer. The sample pulses of the timing generator are divided by 3 by F.F.s 1 and 2 and the output pulses are counted in the ripple counter (F.F.s 4 to 13). The ripple counter is advanced by one after one complete revolution, during which time a set of orthogonal components of the magnetic field is loaded in the three registers. This counter counts the number of samples accumulated in the registers. When the programmed 2^i number is reached, a pulse is transmitted via the gate with

the $\overline{M}_i$ term in it. This pulse sets the clock time delay, F.F. 14, the next clock pulse will set F.F. 4 via G3 and the emitter follower and F.F. 15 which enables G1 and G2 thus starting the "shift i" operations.

F.F. 16 and gates G1 and G2 generate the biphase clock; one phase resets the odd F.F.s and the other phase the even F.F.s of the counter. With this artifice the ripple counter is operated as a ring counter, where the "1" written in the first F.F. is transmitted to the next F.F. upon application of the first reset pulse and is advanced by one position at each successive clock pulse, until it reaches the i position. Then the gate with $\overline{M}_i$ gives a pulse via G4 to reset the counter and sets F.F. 17 to enable the readout by telemetry via G5 and F.F. 20. The next incoming word gate 1 and 2 will set F.F. 20 letting the bit sync pulses go through G6 transmitting out the content of the registers. When the readout is completed F.F.s 20 and 17 are reset via G7 and F.F. 18 is set to "1" initiating the "clear" operation. One clock pulse from H resets the "clear control F.F." and sets F.F. 19 to enable clear pulses to go through G8. When clear is completed X18 will reset F.F. 19 interrupting the clear pulses.

CIRCUITRY AND FABRICATION

The entire digital portion of the experiment is built using a set of standard logic elements using complementary transistor inverters and diode gating. The flip flop circuits used are quite similar to those generally in use by the Instrumentation Section except for their much lower power consumption (150μ watts). The gates used are both positive and negative "and's" and "or's" with inversion.

The A/D converter and timing generator use a low power (25 mw) high gain (50,000) operational amplifier designed at GSFC.

The entire system is packaged using cordwood welded wire techniques, utilizing TO 46 case transistors and glass micro diodes. The right volume and power requirements of the entire system are 5.2 lbs, 120 cu.in. and 0.7 watts, respectively.

SUMMARY

This document has described the technical details of the NASA-GSFC magnetic field instrument on the Pioneer 6, 7 and 8 spacecraft. The scientific results and their interpretation have been presented in a number of publications to date; and listed below:

Burlage, L. F. "Directional discontinuities in the Interplanetary magnetic field," and external report X-616-68-224, submitted to Solar Physics.

Burlage, L. F. "Micro-Scale Structures in the interplanetary medium," Solar Physics, 4, 67, 1968.

Burlage, L. F. and N. F. Ness, "Macro and Micro structure of the Interplanetary Magnetic field," Canadian J. Physics, 46, 5962, 1968.

Fairfield, D. H. "Simultaneous Measurements on three satellites and observation of the Geomagnetic tail at 1000 R_E," an external report, X-612-68-124, JGR, 73, 1968.

N. F. Ness, "Direct measurements of Interplanetary Magnetic field and plasma" an external report X-612-67-293. To be published in Annals IQSY, 1968.

K. W. McCracken, U. R. Rao and N. F. Ness, "The Interrelationship of Cosmic Ray Anisotropies and the interplanetary magnetic field" an external report X-612-67-584, JGR, 73, 1968.

N. F. Ness, C. S. Scearch and S. C. Cantarano, "Probable Observation of the Geomagnetic tail and 10^3 R_E by Pioneer 7," an external report X-612-67-183, JGR, 72, 3769-3776, 1967.

Sari, J. M. and N. F. Ness, "Power Spectra of the interplanetary Magnetic Field," an external report X-616-68- . To be published in Solar Physics.

REFERENCES

Alldredge, U. S. Patent 2,856,581, Magnetometer, October 1958.

Bauernschub, Jr., J. P., Nonmagnetic, Explosive Actuated Indexing Device, National Aeronautics and Space Administration, G-784, 1966.

Geyger, W. A., New Type of Fluxgate Magnetometer, J. App. Phys., Vol. 33, pp. 1280-1281, March 1962.

Gozorth, R. M., Ferromagnetism, D. Van Nostrand, 1951.

Hughes and Sons, U. S. Patent 529,241, Improved Means for the Detection and Measurement of Magnetic Fields, September 1947.

Ness, N. F., C. S. Scearce and S. C. Cantarano, Preliminary Results from the Pioneer 6 Magnetic Field Experiment, J. Geophys. Res., 71, 3305-3313, 1966.

Palmer, T. M., A small Sensitive Magnetometer, Proc. IEEE (London), Vol. 100, pp. 545, 1953.

Schonstedt, U. S. Patent 2,981,885, Saturable Measurements Device and Core Therefore, April 1961.

TRW Systems, Pioneer Project, Flight C, December 8, 1967.

LIST OF TABLES

LIST OF FIGURES

TABLE I

ORBITAL PARAMETERS

	PIONEER		
	6	7	8
LAUNCH	12/16/65 0731 UT	8/11/66 1520 UT	12/13/67 1408 UT
APHELION	0.9866 AU	1.1250 AU	1.0880 AU
PERIHELION	0.8143 AU	1.010 AU	0.9892 AU
INCLINATION	0.1693°	0.09767°	0.0578°
PERIOD	311.3 Days	402.9 Days	386.6 Days
DISTANCE @ SYZYGY			
EARTH TO SPACECRAFT @ SYZYGY	---	808.6 R_E	463.6 R_E
FROM ECLIPTIC PLANE		+23.6 R_E	+8.6 R_E

TABLE II

MAIN SCIENTIFIC FORMATS

Word	Scientific Format A	Scientific Format B	Special Purpose Format D
1	Frame Sync, 7 bits: 1110010	Frame Sync, 7 bits: 1110010	Frame Sync, 7 bits: 1110010
2	Format/Mode Ident. Bit — State 0 1 — Ident. 1 No Yes Format A 2 No Yes Format B 3 No Yes Format C 4 No Yes Format D 5 No Yes Duty Cycle Store 6 No Yes Telemetry Store 7*	Format/Mode Ident. Bit — State 0 1 — Ident. 1 No Yes Format A 2 No Yes Format B 3 No Yes Format C 4 No Yes Format D 5 No Yes Duty Cycle Store 6 No Yes Telemetry Store 7*	Format/Mode Ident. Bit — State 0 1 — Ident. 1 No Yes Format A 2 No Yes Format B 3 No Yes Format C 4 No Yes Format D 5 0 --- 6 RT MRO Mode 7*
3	Scientific Subcom (16 words)	Scientific Subcom (16 words)	Scientific Subcom (16 words)
4	Cosmic Ray (Chicago)	Cosmic Ray (Chicago)	
5			
6	Magnetometer (GSFC)	Magnetometer (GSFC)	
7			
8			
9			
10	Cosmic Ray (Chicago)	Cosmic Ray (Chicago)	
11			
12	Cosmic Ray (GRCSW)		
13	Radio Propagation (Stanford)		Radio Propagation (Stanford)
14		Plasma (MIT)	
15	Plasma (MIT)		
16			
17	Frame Sync Complement 7 bits: 0001101	Frame Sync Complement 7 bits: 0001101	Frame Sync Complement 7 bits: 0001101
18	Subcom Identification 6-bit counter	Subcom Identification 6-bit counter	Subcom Identification 6-bit counter
19	Engineering Subcom (64 words)	Engineering Subcom (64 words)	Engineering Subcom (64 words)
20	Cosmic Ray (Chicago)	Cosmic Ray (Chicago)	
21			
22		Magnetometer (GSFC)	
23			
24			
25			
26	Plasma (ARC)	Cosmic Ray GRCSW	
27			
28			
29		Radio Propagation (Stanford)	Radio Propagation (Stanford)
30			
31		Plasma (ARC)	
32			

*Bit 7 is 0 (zero) for first 32 words of subcommutator and 1 for last 32 words of subcommutator.

TABLE III

ENGINEERING AND ENGINEERING SUBCOMMUTATOR FORMAT, FORMAT C

Word	(a) Bit	State 0	State 1	Identification (b)	Word	(a) Bit	State 0	State 1	Identification (b)
201c	1-7			Frame Sync, 1110010	214	92-97			Not Assigned
202c	8	No	Yes	Format A	215	99-105			Spacecraft Spin, revs/64 sec
	9	No	Yes	Format B	216	106-111			TWT No. 1 Anode Voltage
	10	No	Yes	Format C	217c	113-119			Frame Sync Complement, 0001101
	11	No	Yes	Format D	218	120-125			Rcvr. No. 1 Static Phase Error
	12	No	Yes	Duty Cycle Store	219	127-132			Rcvr. No. 2 Static Phase Error
	13	No	Yes	Telemetry Store	220	134-139			Rcvr. No. 1 Signal Strength
	14	Yes	No	First 32 Words of Format C	221	141-146			Rcvr. No. 2 Signal Strength
203	15-20				222	148-153			Rcvr. No. 1 and 2 Temperature
204	22-27				223	155-160			TWT No. 1 Helix Current
205	29	No	Yes	Bit Rate, 512 bps	224	162-167			TWT No. 1 Cathode Current
	30	No	Yes	Bit Rate, 256 bps	225	169-174			TWT No. 2 Helix Current
	31	No	Yes	Bit Rate, 64 bps	226	176-181			TWT No. 2 Cathode Current
	32	No	Yes	Bit Rate, 16 bps	227	183-188			TWT No. 1 Temperature
	33	No	Yes	Bit Rate, 8 bps	228	190-195			TWT No. 2 Temperature
	34	Yes	No	Interlock Switch to Orient. Elect.	229	197-202			TWT Converter Temperature
206	36	Off	On	Battery Power	230	204-209			Driver Temperature
	37			Orient. Press. Switch Actuated	231	211-216			DTU Temperature
	38	Off	On	Orientation Power	232	218-223			DSU Temperature
	39	Yes	No	Undervoltage Protection in Effect	233c	225-231			Frame Sync, 1110010
	40	No	Yes	Voltage Below Switch Trip Level	234c	232	No	Yes	Format A
	41	B	A	DTU Redundancy		233	No	Yes	Format B
207	43	2	1	Antennas to TWT Number		234	No	Yes	Format C
	44	Low	High	TWT to Gain of Antenna		235	No	Yes	Format D
	45	Ant	TWT's	Driver to		236	No	Yes	Duty Cycle Store
	46	Driver	TWT's	Low Gain Antenna to		237	No	Yes	Telemetry Store
	47	Off	On	TWT No. 1 Power		238	No	Yes	Last 32 Words of Format C
	48	Off	On	TWT No. 2 Power	235	239-244			Experiment A D4 Voltage
208	50	Off	On	Converter No. 1 +16 volts	236	246-251			Experiment A Temperature
	51	Off	On	Converter No. 1 +10 volts	237	253-258			DTU A/D Converter Calib. No. 1
	52	On	Off	Converter No. 1 -16 volts	238	260-265			DTU A/D Converter Calib. No. 2
	53	Off	On	Converter No. 2 +16 volts	239	267-272			DTU A/D Converter Calib. No. 3
	54	Off	On	Converter No. 2 +10 volts	240	274-279			Equipment Converter +16-volt Bus
	55	On	Off	Converter No. 2 -16 volts	241	281-286			Equipment Converter +10-volt Bus
209	57	No	Yes	Decoder No. 1 Signal Present	242	288-293			Equipment Converter -16-volt Bus
	58	No	Yes	Decoder No. 2 Signal Present	243	295-300			Equipment Converter 1 & 2 Temp.
	59	Yes	No	Rcvr. No. 1 Signal Present	244	302-307			Bus Voltage
	60	Yes	No	Rcvr. No. 2 Signal Present	245	309-314			Bus Current
	61	Low	High	Rcvr. No. 2 to Gain of Antenna	246	316-321			Battery Temperature
	62	Off	On	Coherent Mode	247	323-328			Battery Current
210	64	No	Yes	Ordnance System Armed	248	330-335			TWT No. 2 Anode Voltage
	65	No	Yes	3rd Stage Separated	249c	337-343			Frame Sync Complement, 0001101
	66	Yes	No	Boom No. 1 (Orientation) Deployed	250	344-349			Forward Solar Panel Temperature
	67	Yes	No	Boom No. 2 (Magnetometer) Deployed	251	351-356			After Solar Panel Temperature
	68	Yes	No	Boom No. 3 (Wobble Damper) Deployed	252	358-363			Platform Temperature (No. 2)
	69	Yes	No	Stanford Antenna Deployed	253	365-370			Boom Bracket Temperature
211	71	On	Off	Experiment B Power	254	372-377			High-Gain Ant. Mount. Bracket Temp.
	72			Not Assigned	255	379-384			Louver Actuator Housing Temperature
	73			Not Assigned	256	386-391			Sun Sensor A Temperature
	74	On	Off	Experiment C Power	257	393-398			Platform Temperature (No. 1)
	75	No	Yes	Experiment C Acquiring Data	258	400-405			Nitrogen Bottle Pressure
	76	2	1	Experiment C Mode	259	407-412			Nitrogen Bottle Temperature
212	78	On	Off	Experiment A Power	260	414-419			Not Assigned
	79	No	Yes	TS Mode Signal to Experiment A	261	421-426			Not Assigned
	80			Not Assigned	262	428-433			Sun Sensor C Temperature
	81	On	Off	Experiment G Power	263	435-440			Platform Temperature (No. 3)
	82			Not Assigned	264	442-447			Experiment B Temperature
	83			Not Assigned					
213	85	On	Off	Experiment D Power, 28 volts					
	86	No	Yes	Experiment D Calibrate Mode					
	87	Off	On	Experiment D Dynamic Range					
	88	No	Yes	Experiment D Data Overflow					
	89	Off	On	Experiment D Power, 12 volts					
	90	On	Off	Experiment E Power					

(a) There are seven telemetry bits in each telemetry channel. Bits are numbered from 1 to 448 in the order they will be received from the spacecraft. Bit numbers missing in sequence refer to bits used to indicate parity (odd) for the first third and fifth bits. For analog and digital words, the first bit received is the "most significant bit."

(b) Pioneer VI experiments are identified by letters as follows:

A - University of Chicago Cosmic Ray Experiment
B - GSFC Magnetometer
C - MIT Plasma Experiment
D - GRCSW Cosmic Ray Experiment
E - Stanford University Radio Propagation Experiment
G - ARC Plasma Experiment

(c) Word not assigned when subcommutated.

TABLE IV

SCIENTIFIC SUBCOMMUATOR FORMAT, FORMAT E

Word	Type	Identification
101	Digital	Cosmic Ray (Chicago)
102	Analog	Radio Propagation (Stanford)
103	Digital	Unassigned
104	Digital	
105	Digital	
106	Digital	
107	Analog	Radio Propagation (Stanford)
108	Analog	Plasma (ARC)
109	Digital	Cosmic Ray (Chicago)
110	Digital	Plasma (MIT)
111	Analog	Radio Propagation (Stanford)
112	Analog	Plasma (ARC)
113	Digital	Magnetometer (GSFC)
114	Digital	
115	Analog	Radio Propagation (Stanford)
116	Digital	

	Bit Rate					
	512	256	64	16	8	
Bit 1	1	0	0	1	0	Identification
Bit 2	0	1	0	1	1	
Bit 3	0	0	1	0	1	
Bit 4	Most Significant Bit					Extended Frame Counter
Bit 5						
Bit 6						
Bit 7	Least Significant Bit					

TABLE V

SPACECRAFT MODES OF OPERATION

1. Real-Time Mode. Data transmitted directly without intermediate storage at bit rate selected by ground command.

2. Memory Readout Mode. Data readout from storage and transmitted at bit rate selected by ground command.

3. Telemetry Storage Mode. Data stored and transmitted simultaneously and continuously until storage unit is full. Upon filling of storage unit, the data handling subsystem shall revert automatically to real-time mode at bit rate of 16 bps in Format B.

4. Duty Cycle Storage Mode. Intermittent storage of one frame at a rate of 512 bps. Two engineering frames are interlaced with eight scientific frames. The time increments between frames stored and the total time to fill the storage unit will be selected by ground command as follows:

Time Between Frames Stored	Approximate Time to Fill Storage
2 min. 8 sec.	2.30 hours
4 min. 16 sec.	4.77 hours
8 min. 32 sec.	9.54 hours
17 min. 4 sec.	19.07 hours

Upon filling the data storage unit, the data handling subsystem will revert automatically to the real-time mode at a bit rate of 16 bps in Form B.

TABLE VI

EXPERIMENT DATA FORMAT

The information is recorded as three 8 bit words from least significant to most significant reading from right to left and in the order D_1, D_2, D_3. The information however, is telemetered as four 7 bit words (6 bits of information +1 bit parity) in the order D_3, D_2, D_1 starting with the least significant bit of D_3 and ending with the most significant bit of D_1.

RECORDED

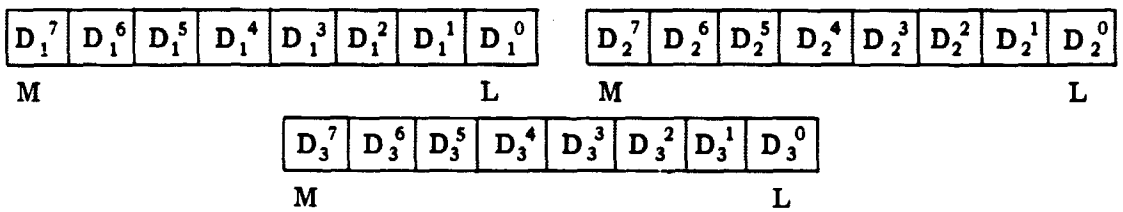

TELEMETERED

FORMAT A

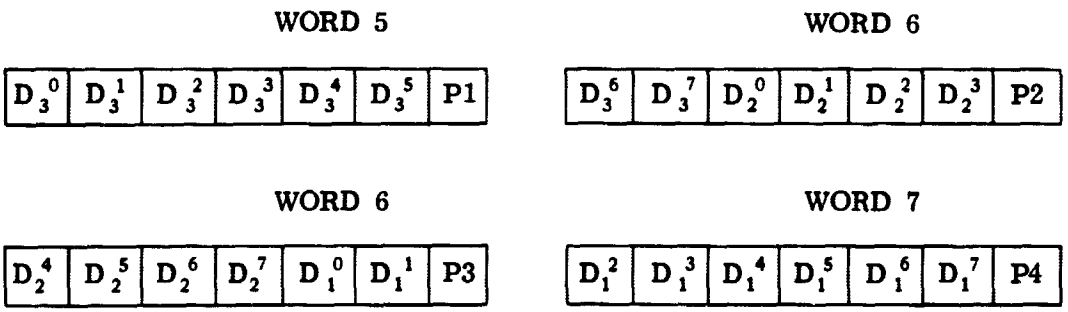

FORMAT B

Words 5, 6, 7, and 8 are the same as format A. Words 21, 22, 23 and 24 are the same as words 5, 6, 7, and 8.

TABLE VII

AVERAGING TIME COMPARED TO TRANSMISSION

TIME AT 60 RPM

REAL TIME TRANSMISSION

BIT RATE	AVERAGING TIME	NO. OF SAMPLES	TIME BETWEEN READOUT
16 BPS	4 sec.	2^2	7 sec.
8 BPS	8 sec.	2^3	14 sec.

DUTY CYCLE STORAGE MODE

512 or 256 BPS	1 min. 4 sec.	2^6	2 min. 8 sec.
64 BPS	2 min. 8 sec.	2^7	4 min. 16 sec.
16 BPS	4 min. 16 sec.	2^8	8 min. 32 sec.
8 BPS	4 min. 16 sec.	2^8	17 min. 4 sec.

TABLE VIII

GROSS PROPERTIES - PIONEER SPACECRAFT

	A-6669 Spec.	6	7	8
Weight (lb.)				
Spacecraft	111.2	102.7	103.26	106.0
Experiment		34.3	35.09	38.1
Total		137.0	138.35	144.1
Moments (lb. in^2) (deployed)				
Roll		43509	43509	45620
Pitch-max.		32115	32115	33120
Ratio (Roll/Pitch)		1.32	1.32	1.38
Electrical Loads (watts)				
Spacecraft		43.4	43.6	43.1
Experiments (average)	7.4	9.2	8.2	12.3
Total		52.6	51.8	55.4
Solar Array (watts) Capacity				
0.8 AU	S/C loads	102.5	97.8	96.5
1.0 AU	plus 7.4w	81.0	80.6	79.5
1.2 AU	for exper.	60.2	60.8	60.0
Magnetic Properties (gamma) (with experiments)				
As Received		.17	.239	.14
Magnetized	16	1.68	1.46	1.97
Demagnetized	1.0	0.051*	.23	.14
Stray Field	0.5	0.120	.337	.16
Experiment Mounting Temperature (°F)				
0 [illegible]	30-90	75-80	83	84 (Minn.)
Temperature (°F)				
1.0 AU**	30-90	62	62	54
1.2 AU**	30-90	41	38	41
RF Power to Antenna (dbm)				
Low Gain	+36	+37	+36.7	37.4
High Gain	+36	+38	+37.5	38.0
Radiating Antenna Gain (db)				
Low Gain		-0.5	+ .3	- .4
High Gain		+10.9	+10.7	+11.1
Receiver Sensitivity at Antenna (dbm)				
Low Gain	-135	-143	-142.5	-141.1
High Gain	-135	-144	-144.2	-140.3
Receiving Antenna Gain (db)				
Low Gain		- 0.7	- 1.7	- 1.3
High Gain		+10.9	+11.1	+ 11.8

*Based on readings at 50" extrapolated to 80"
**Platform #3 temperature.

TABLE IX

POST FLIGHT ZERO CALIBRATION

PIONEER 6

FLIGHT NO.	DATE	ZERO
#1	12/23/65	119.0
#2	1/7/66	119.0
#3	1/27/66	119.0
#4	3/3/66	119.0
#5	3/31/66	119.0
#6	4/28/66	118.2
#7	5/19/66	118.0
#8	7/14/66	118.8
#9	12/16/66	119.1
	PIONEER 7	
#1	Too noisy	——
#2	9/1/66	134.3
#3	10/7/66	134.2
#4	11/4/66	134.5
#5	2/29/67	134.5
#6	3/1/63	134.7
	PIONEER 8	
		±32γ
#1	12/21/67	116.5
#2	1/25/68	115.4
#3	3/7/68	115.3
#4	6/12/68	111.3
#5	7/17/68	113.0

TABLE X

EXPERIMENT SPECIFICATIONS

	6	7	8
Weight			
Electronic Assembly	4.5 lb	4.5 lb	5.0 lb
Boom Assembly	0.7 lb	0.7 lb	0.7 lb
Power	0.7W	0.7W	0.9W
Input Voltage	28 VDC + 5-4	28 VDC + 5-4	28 VDC + 5-4
Range	$\pm 64\gamma$	$\pm 32\gamma$	$\pm 32\gamma$ & $\pm 96\gamma$
Thermal Calibration			
Electronics		-25°C to +55°C	
Sensor		-75°C to +75°C	
Zero Drift	$<\pm 1$	$<\pm 1$	$<\pm 1$
Resolution (Sensitivity)	$\pm 0.25\gamma$	$\pm 0.125\gamma$	$\pm 0.125\gamma$ & $\pm 0.375\gamma$

TABLE XI

LINEARITY PIONEER 6

γ(DC)	Malibu	GSFC	Best Fit
60	249.5	242.8	246.2
50	228.0	222.6	225.3
40	207.4	201.7	204.6
30	184.8	181.4	183.1
20	164.2	161.4	162.8
10	142.9	140.6	141.8
0	120.4	120.3	120.4
-10	98.3	100.3	99.3
-20	77.5	80.4	78.9
-30	55.4	58.8	57.1
-40	34.6	38.8	36.7
-50	12.7	18.2	15.4
Internal Calibrate	-21.2	-20.6	-20.8
			RMSE $0.2\gamma^2$

LINEARITY PIONEER 7

γ(DC)	Malibu	GSFC	
30	253.1		253.1
25	233.8	239.5	233.8
20	214.0	217.5	214.0
15	194.6	197.7	194.6
10	174.7	176.6	174.7
5	154.8	155.4	154.8
0	134.5	133.5	134.5
- 5	114.6	112.0	114.6
-10	95.0	91.6	95.0
-15	75.0	70.3	75.0
-20	55.6	49.2	55.6
-25	35.6	28.8	35.6
-30	16.2	8.1	16.2
Internal Calibrate	+40.6	+42.2	+40.6
			RMSE $0.1\gamma^2$

LINEARITY PIONEER 8

Low Range ±32

(DC)	Malibu	GSFC	
30	234.3	239.3	234.3
25	216.0	220.1	216.0
20	197.3	200.9	197.3
15	179.3	181.6	179.3
10	160.2	161.9	160.2
5	141.5	141.2	141.5
0	121.6	122.0	121.6
- 5	102.2	100.8	102.2
-10	82.8	82.1	82.8
-15	63.4	60.4	63.4
-20	44.0	42.5	44.0
-25	24.6	21.7	24.6
30	5.2	3.1	5.2
Internal Calibrate	-37.6	-39.5	-37.6

RMSE $0.3\gamma^2$

High Range ±96γ

γ (DC)	Malibu	GSFC	Best Fit
90	246.2	246.4	246.4
80	232.3	232.8	232.6
70	219.4	220.7	219.0
60	208.0	206.8	207.4
50	194.0	193.9	194.0
40	179.9	180.5	180.2
30	167.1	167.1	167.1
20	154.6	153.9	154.2
10	141.7	141.4	141.6
0	128.7	128.0	128.0
-10	115.6	114.5	115.0
-20	102.6	101.1	101.8
-30	89.5	88.8	89.3
-40	76.4	75.8	76.1
-50	63.4	62.7	63.0
-60	50.3	49.6	50.0
-70	37.3	36.6	37.0
-80	24.2	23.5	23.8
-90	11.2	10.5	10.8
Internal Calibrate	-12.7	-12.8	-12.7

RMSE 0.1γ^2

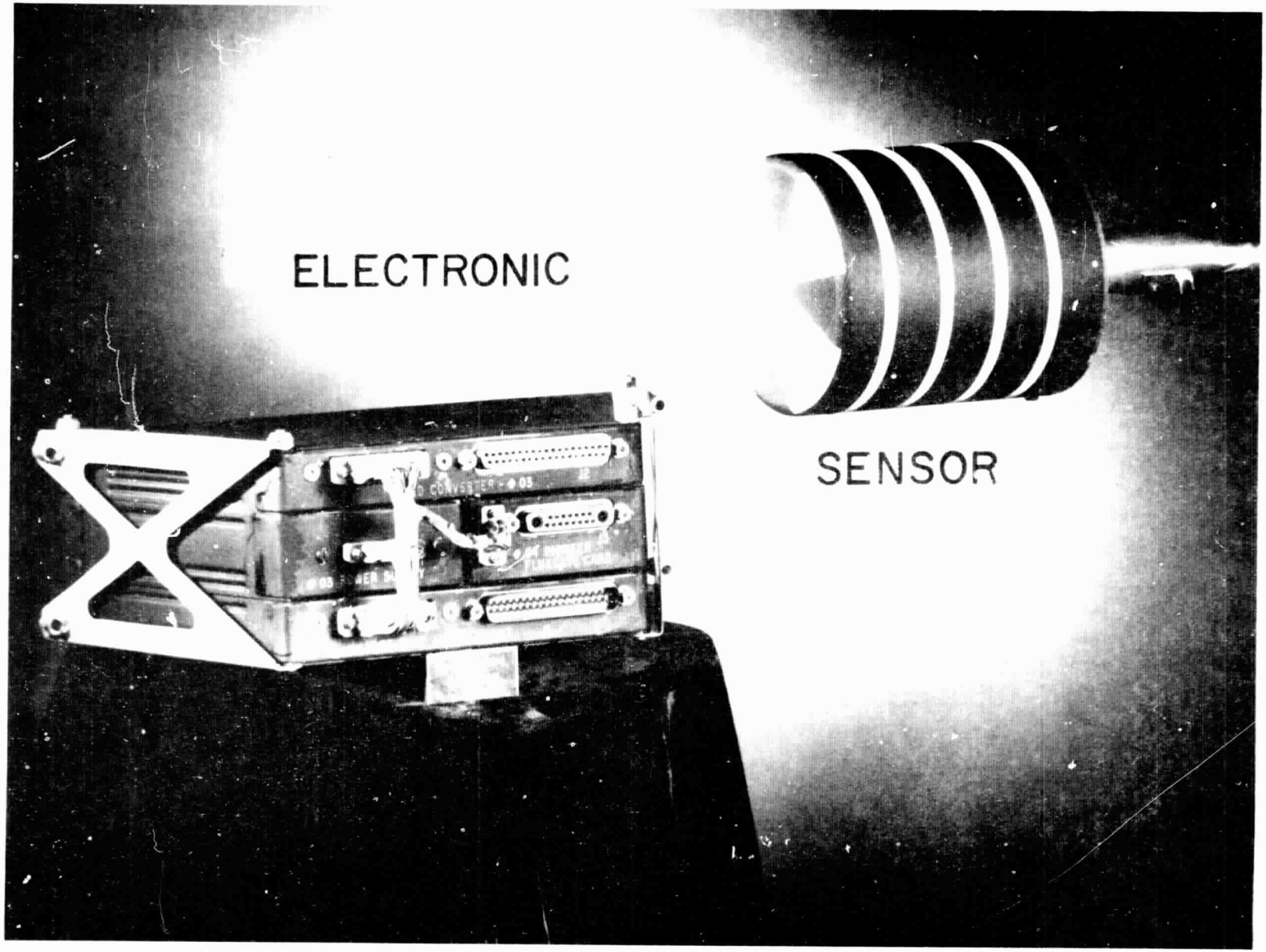

FIG. I

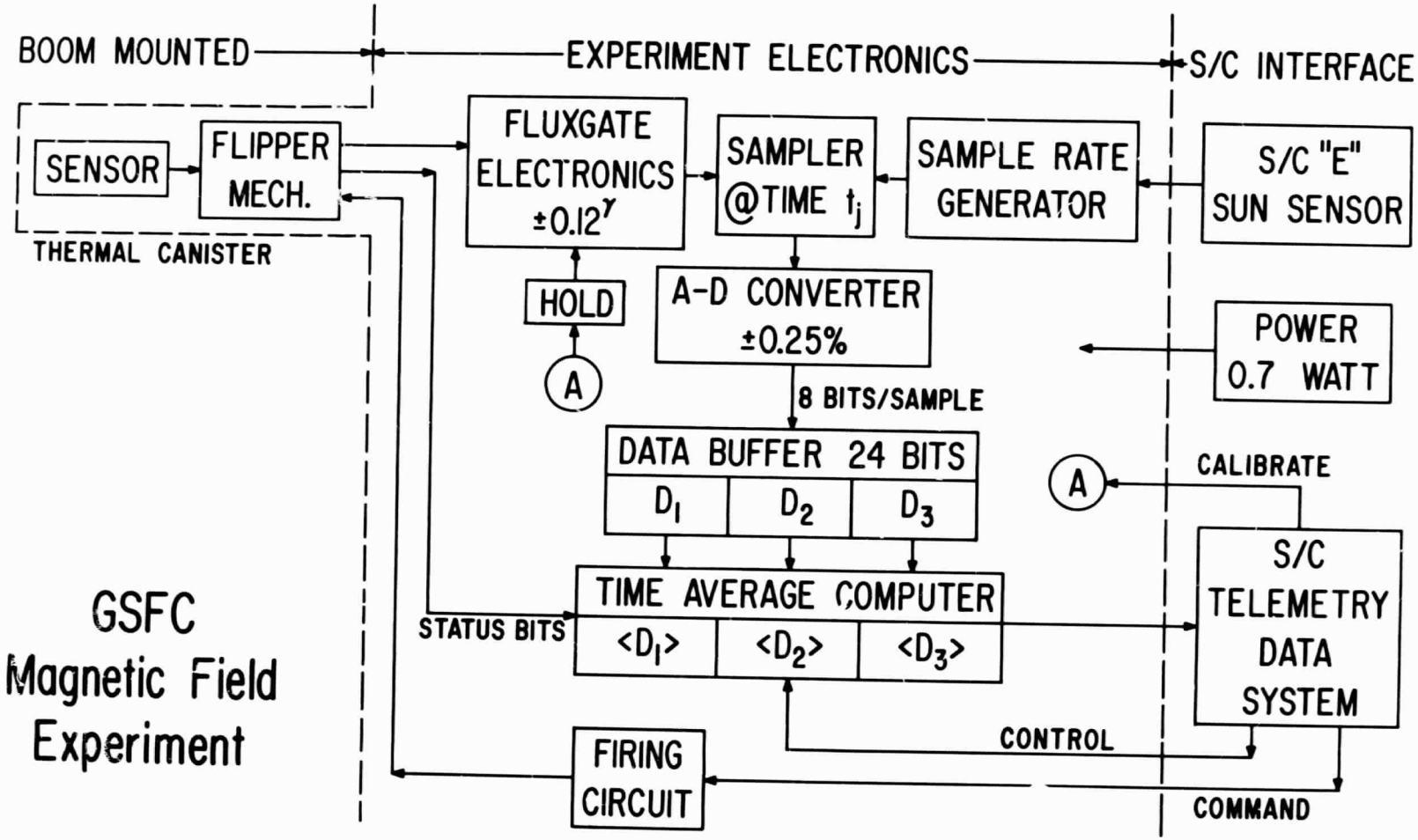
BOOM MOUNTED
EXPERIMENT ELECTRONICS
S/C INTERFACE
SENSOR
FLIPPER MECH.
THERMAL CANISTER
FLUXGATE ELECTRONICS ±0.12γ
SAMPLER @TIME t_j
SAMPLE RATE GENERATOR
S/C "E" SUN SENSOR
HOLD
A
A-D CONVERTER ±0.25%
8 BITS/SAMPLE
POWER 0.7 WATT
DATA BUFFER 24 BITS
D_1 D_2 D_3
A
CALIBRATE
TIME AVERAGE COMPUTER
STATUS BITS
$<D_1>$ $<D_2>$ $<D_3>$
S/C TELEMETRY DATA SYSTEM
CONTROL
FIRING CIRCUIT
COMMAND
GSFC
Magnetic Field
Experiment

FIG. 2

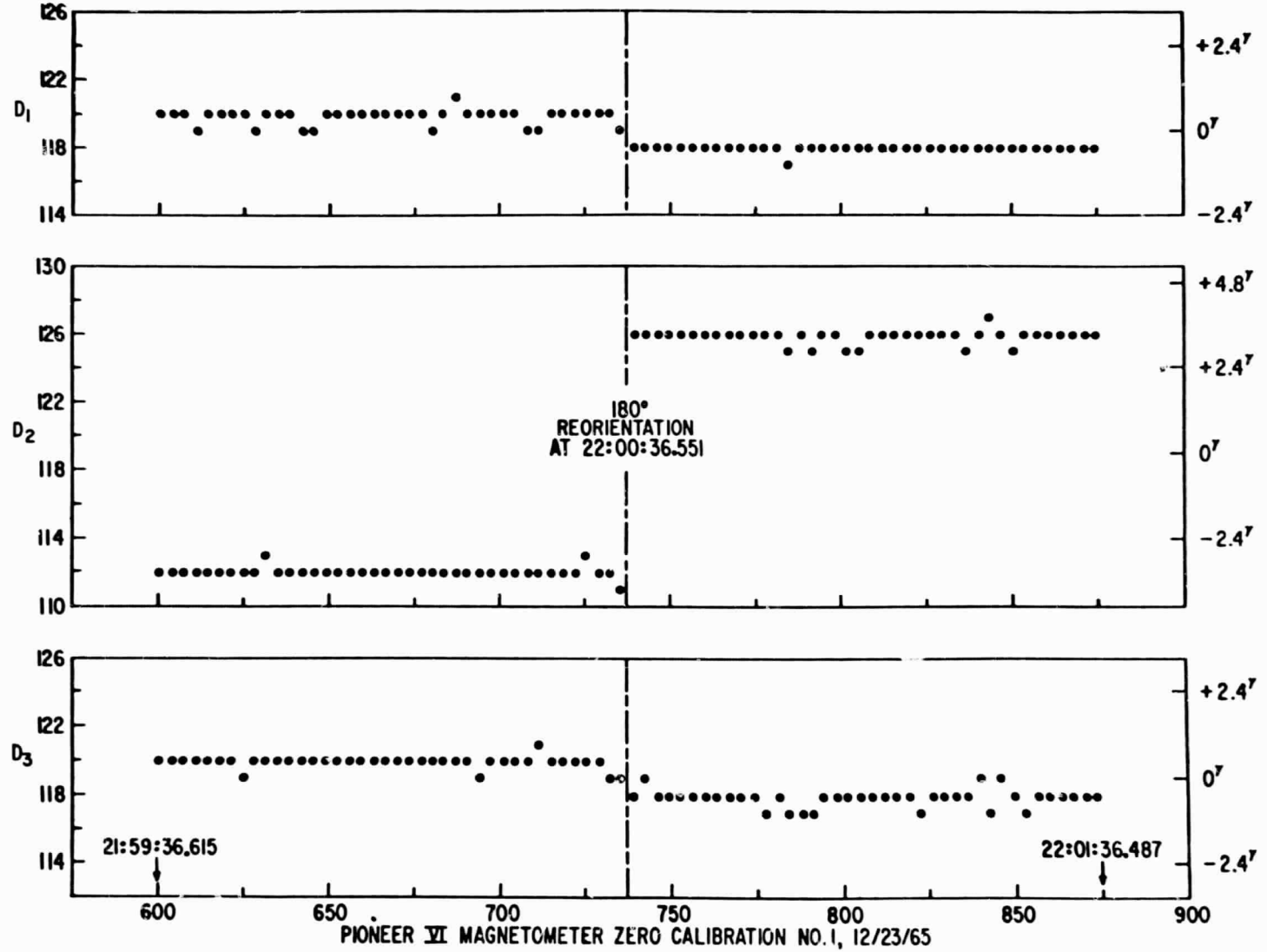
126
122
118
114
D_1
+2.4γ
0γ
-2.4γ
130
126
122
118
114
110
D_2
180°
REORIENTATION
AT 22:00:36.551
+4.8γ
+2.4γ
0γ
-2.4γ
126
122
118
114
D_3
21:59:36.615
22:01:36.487
+2.4γ
0γ
-2.4γ
600
650
700
750
800
850
900
PIONEER VI MAGNETOMETER ZERO CALIBRATION NO.1, 12/23/65

FIG. 3

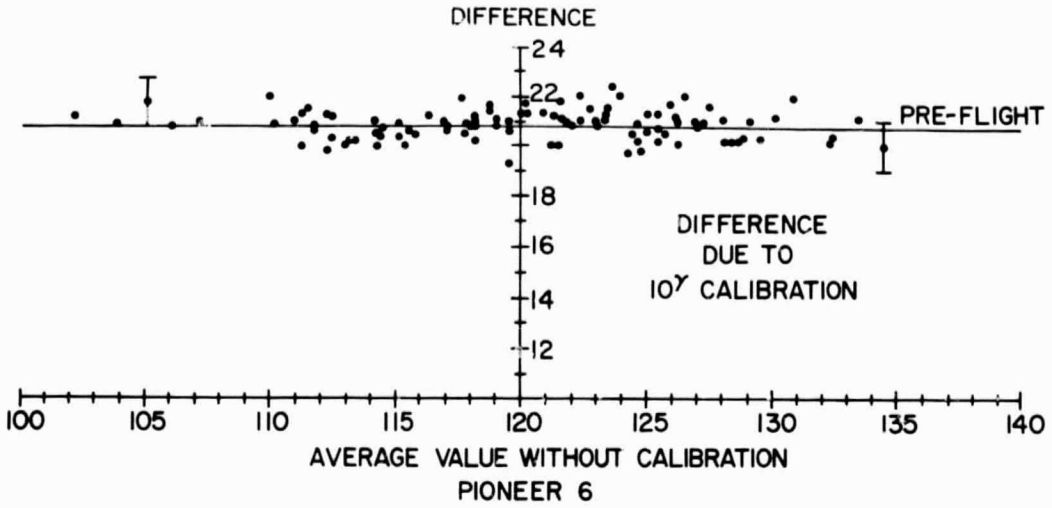
DIFFERENCE
24
22
18
16
14
12
PRE-FLIGHT
DIFFERENCE
DUE TO
10γ CALIBRATION
100 105 110 115 120 125 130 135 140
AVERAGE VALUE WITHOUT CALIBRATION
PIONEER 6

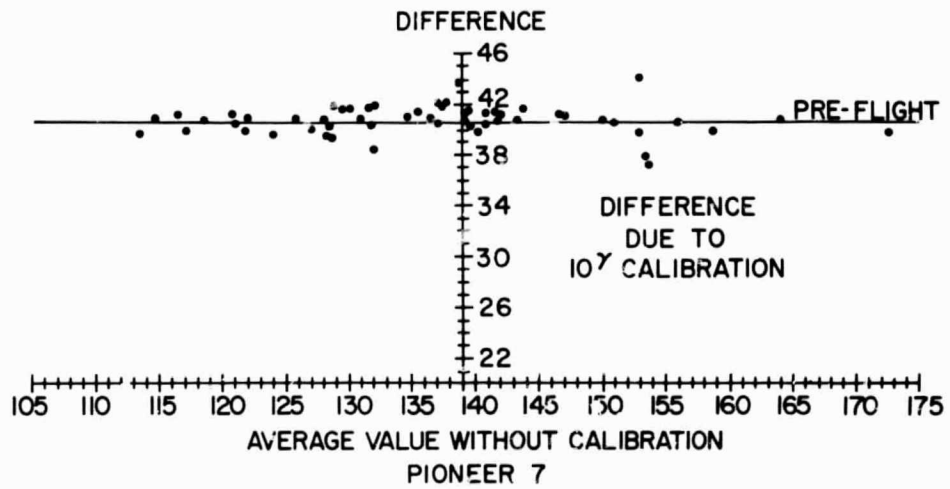
DIFFERENCE
46
42
38
34
30
26
22
PRE-FLIGHT
DIFFERENCE
DUE TO
10γ CALIBRATION
105 110 115 120 125 130 135 140 145 150 155 160 165 170 175
AVERAGE VALUE WITHOUT CALIBRATION
PIONEER 7

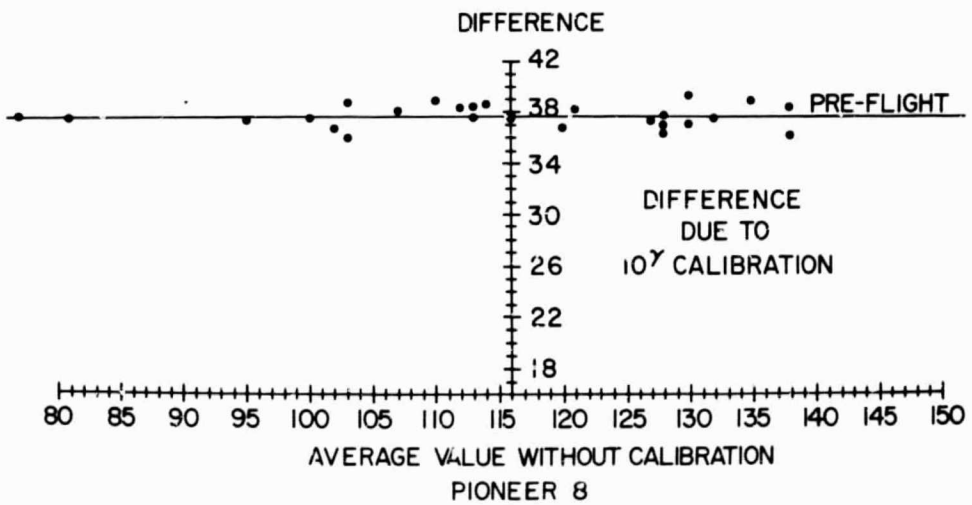
DIFFERENCE
42
38
34
30
26
22
18
PRE-FLIGHT
DIFFERENCE
DUE TO
10γ CALIBRATION
80 85 90 95 100 105 110 115 120 125 130 135 140 145 150
AVERAGE VALUE WITHOUT CALIBRATION
PIONEER 8

FIG.4

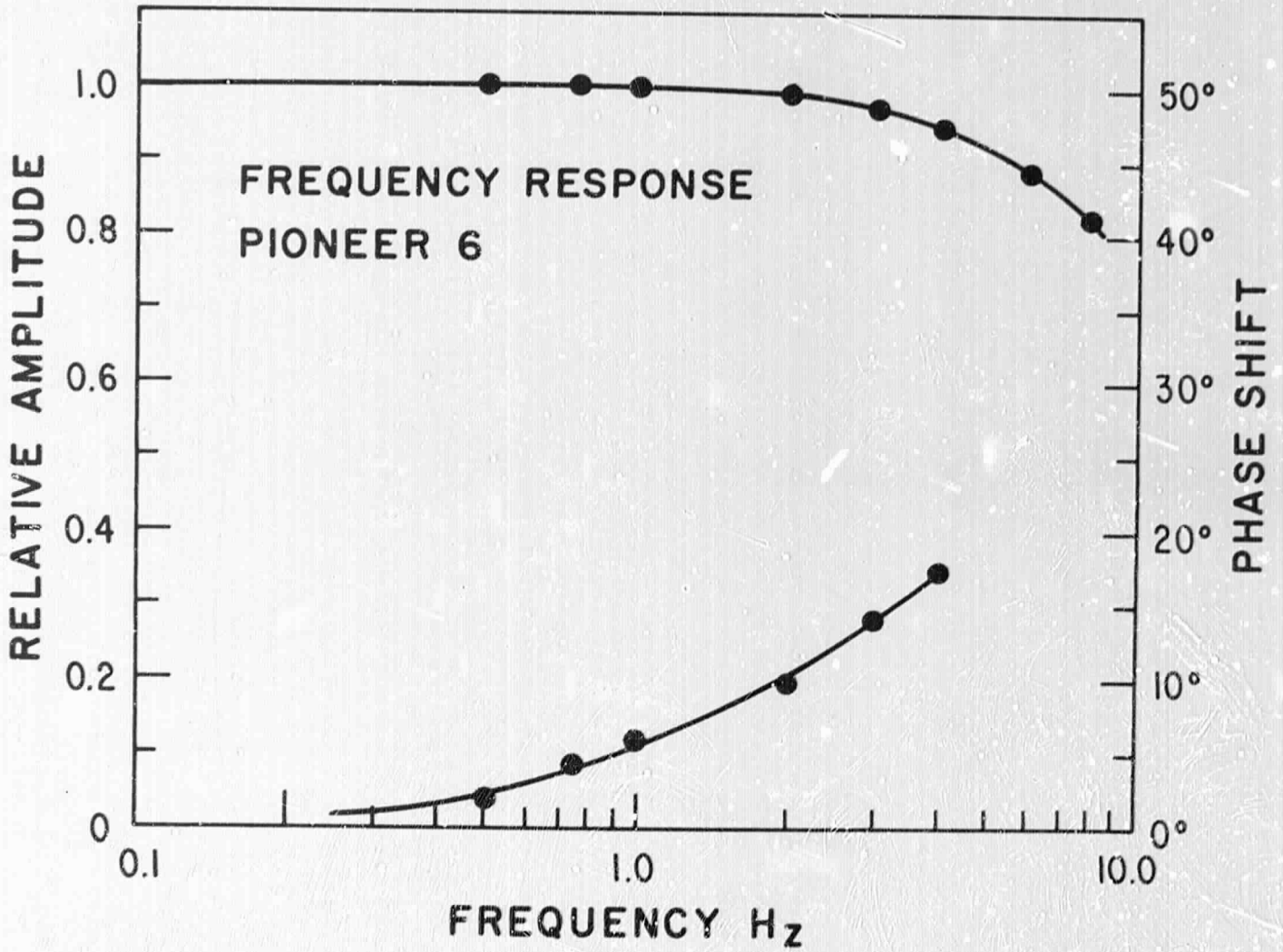
FREQUENCY RESPONSE
PIONEER 6
RELATIVE AMPLITUDE
PHASE SHIFT
1.0
0.8
0.6
0.4
0.2
0
50°
40°
30°
20°
10°
0°
0.1
1.0
10.0
FREQUENCY Hz

FIG. 5(a)

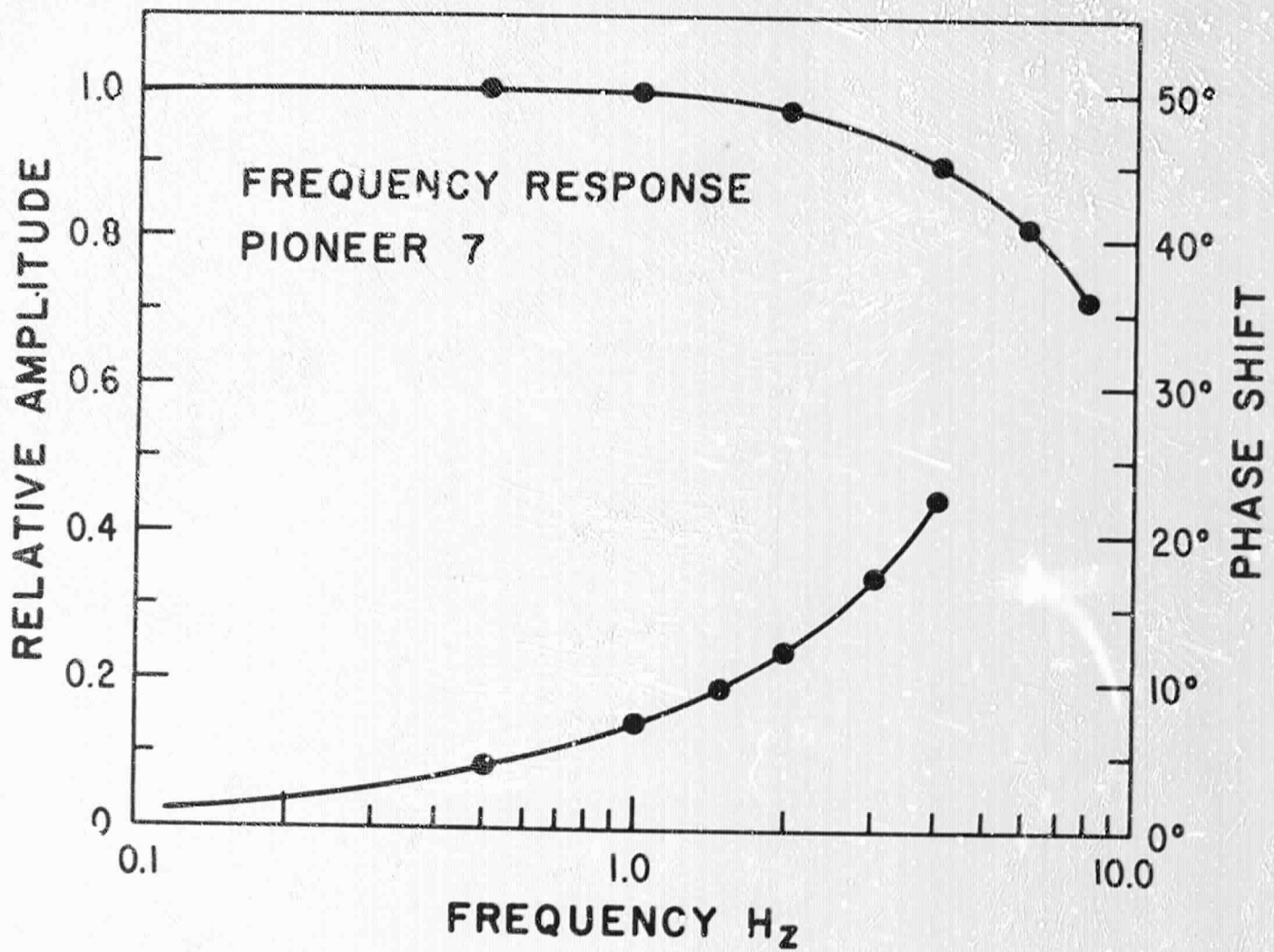
FREQUENCY RESPONSE
PIONEER 7
RELATIVE AMPLITUDE
1.0
0.8
0.6
0.4
0.2
0
PHASE SHIFT
50°
40°
30°
20°
10°
0°
0.1
1.0
10.0
FREQUENCY Hz

FIG. 5 (b)

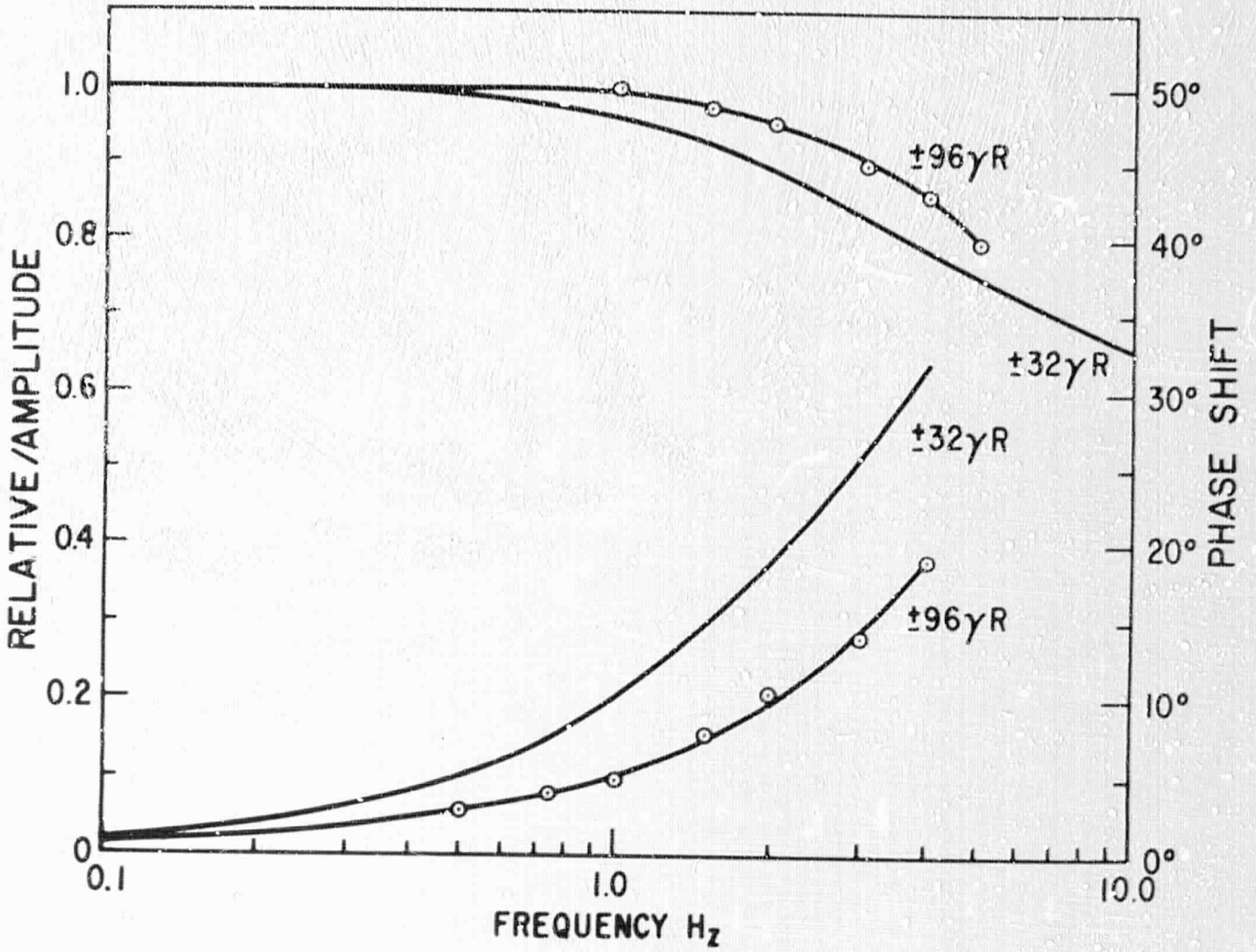

Figure 5(c). Frequency Response Pioneer 8

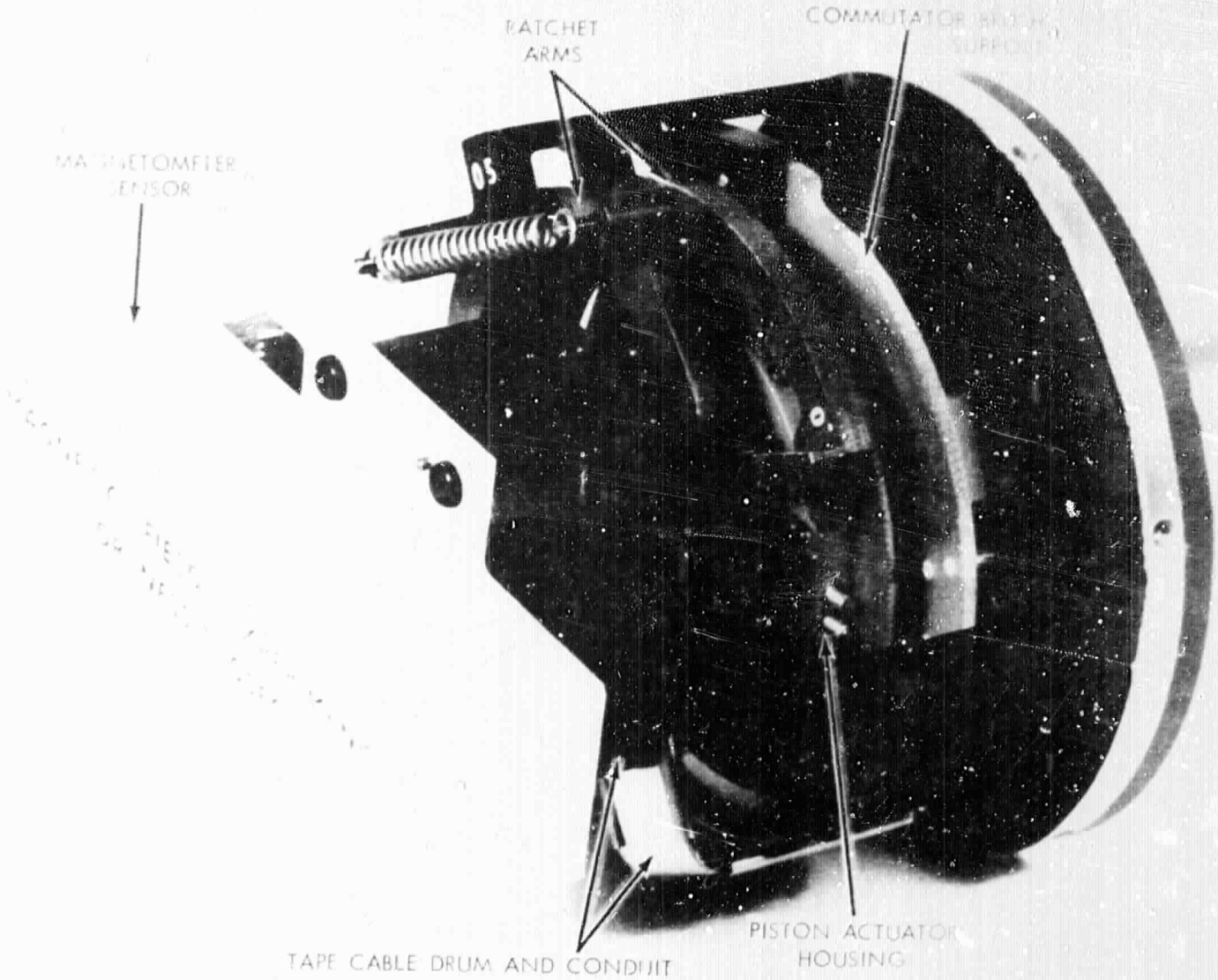
RATCHET
ARMS
COMMUTATOR
PISTON ACTUATOR
HOUSING
TAPE CABLE DRUM AND CONDUIT

FIG. 6

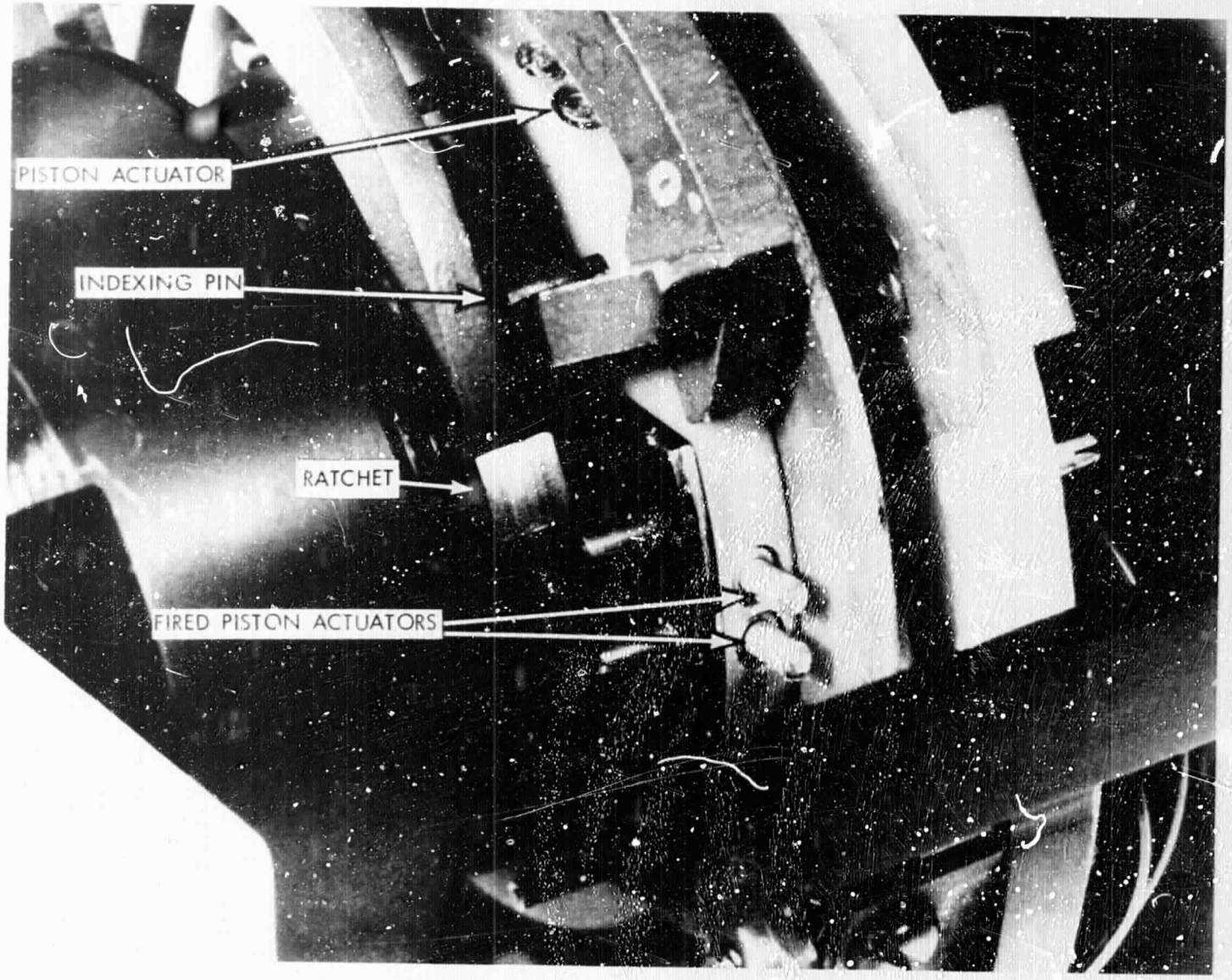
PISTON ACTUATOR
INDEXING PIN
RATCHET
FIRED PISTON ACTUATORS

FIG. 7

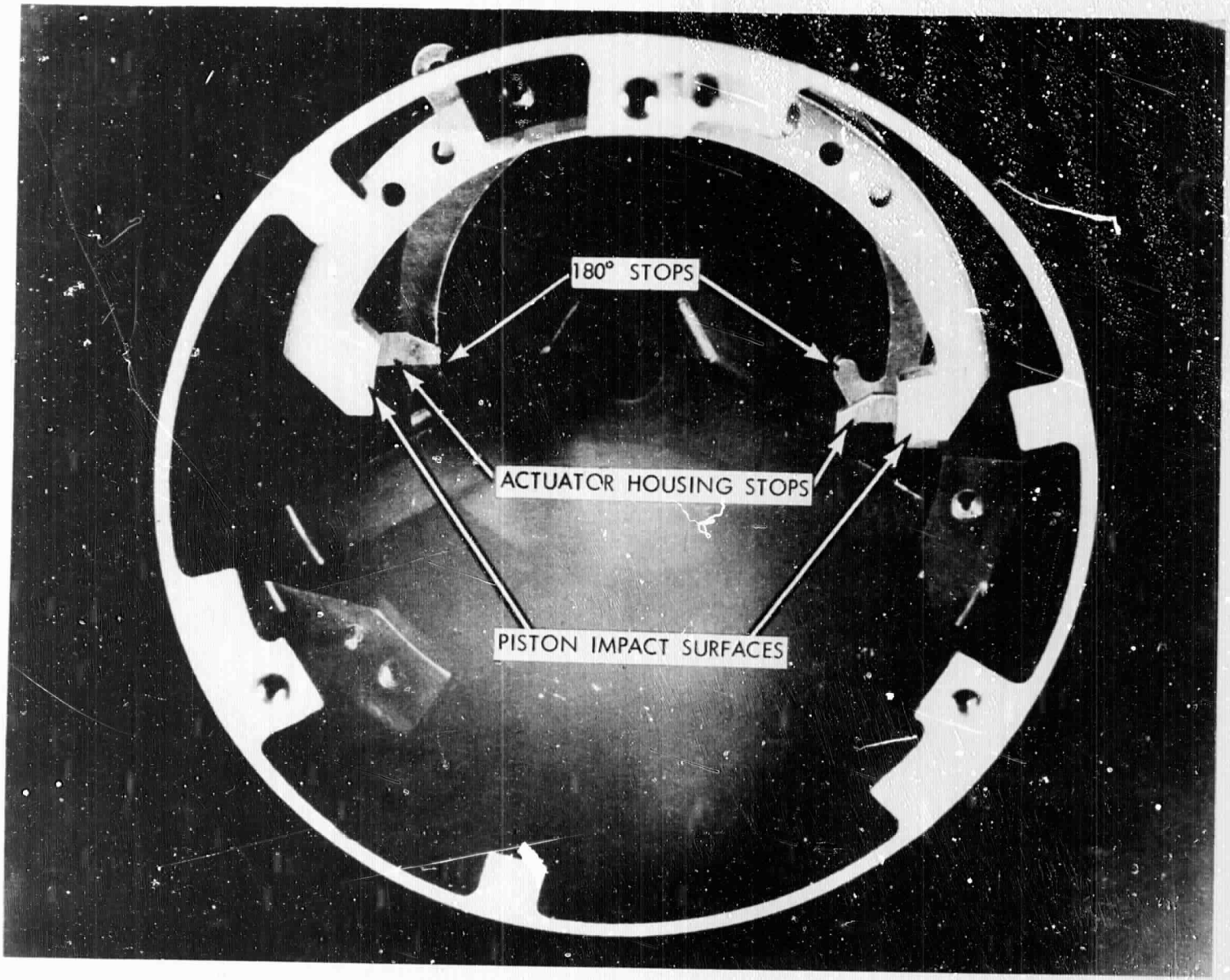

FIG. 8

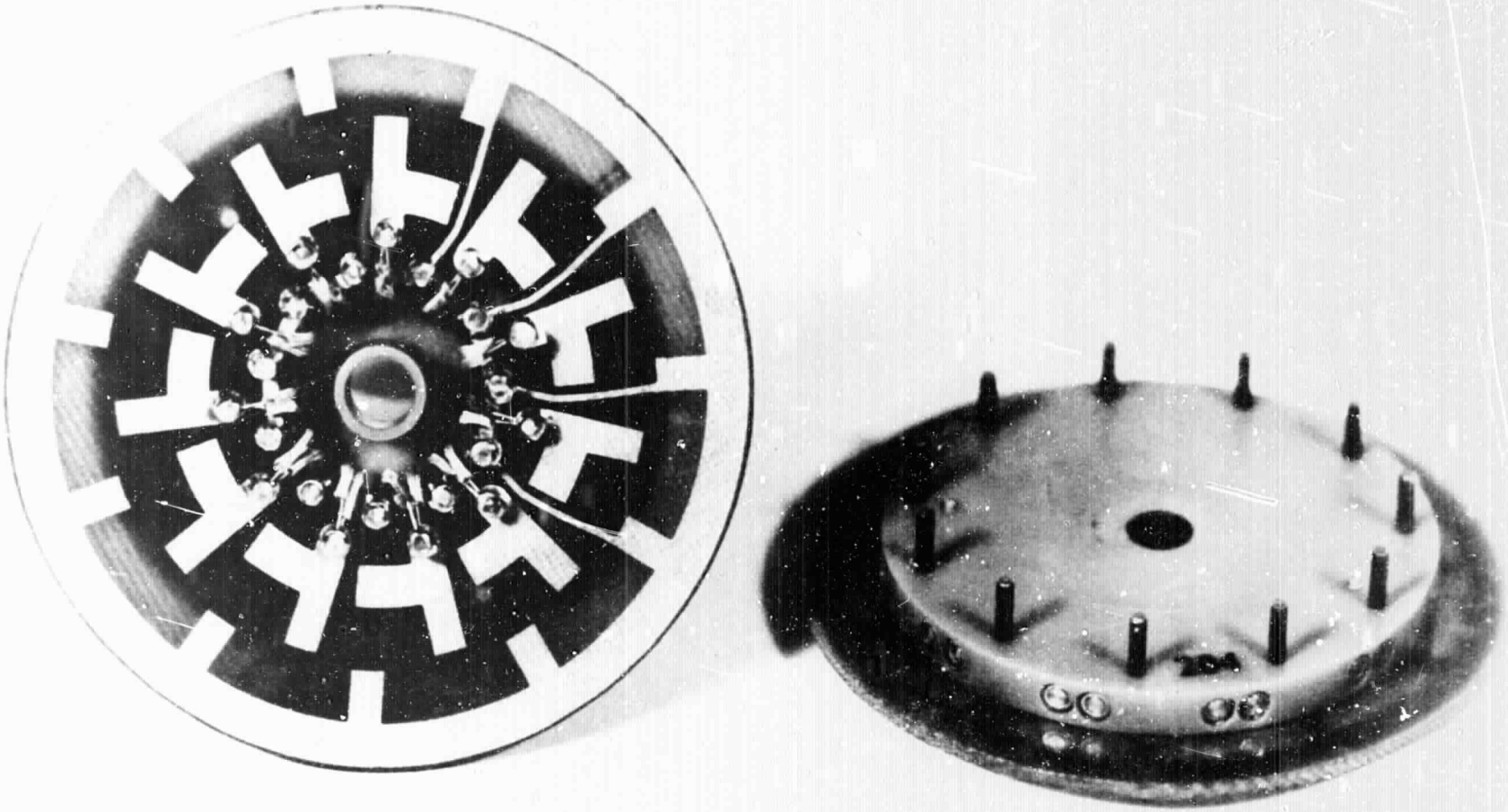

FIG. 9

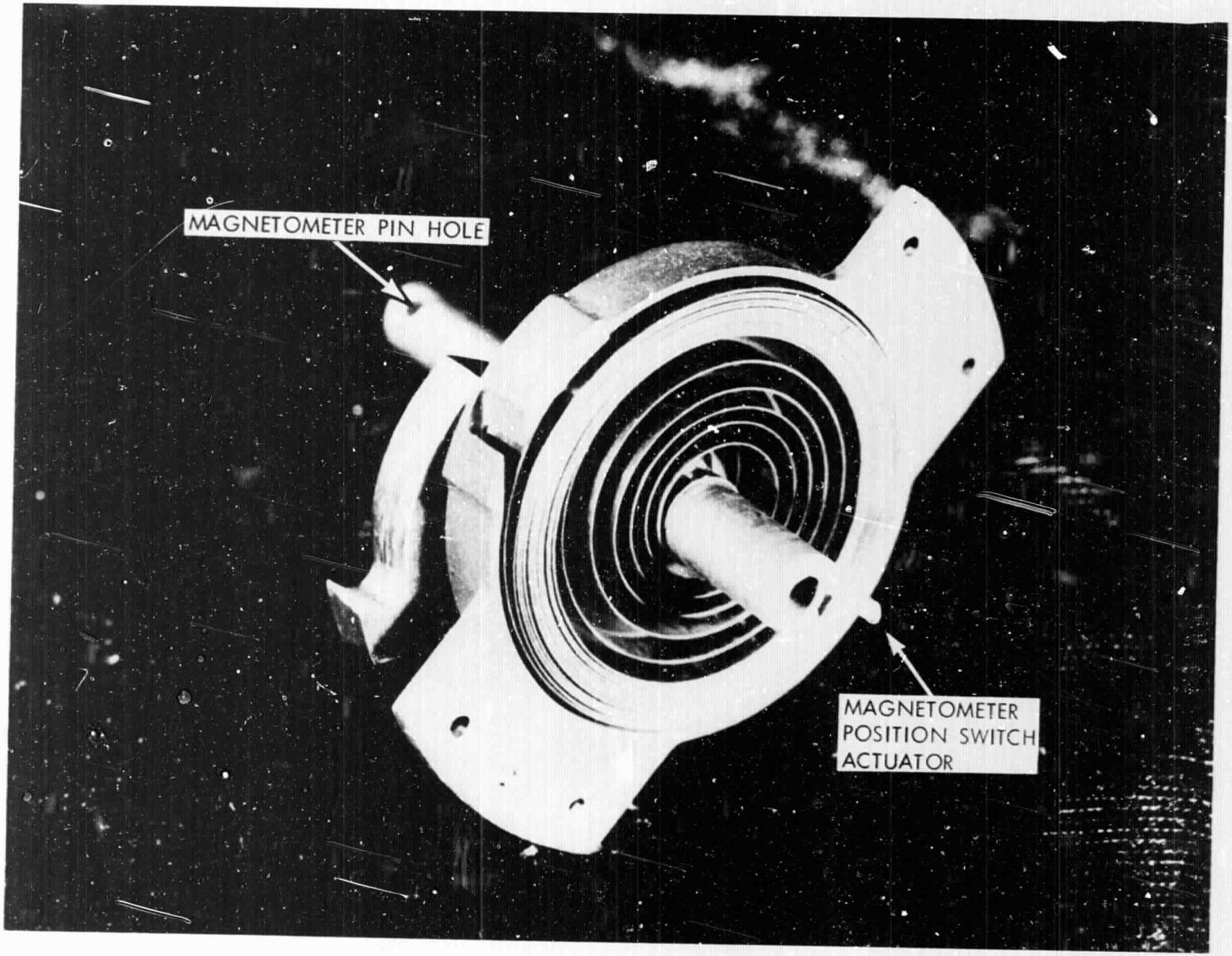
MAGNETOMETER PIN HOLE
MAGNETOMETER
POSITION SWITCH
ACTUATOR

FIG. 10

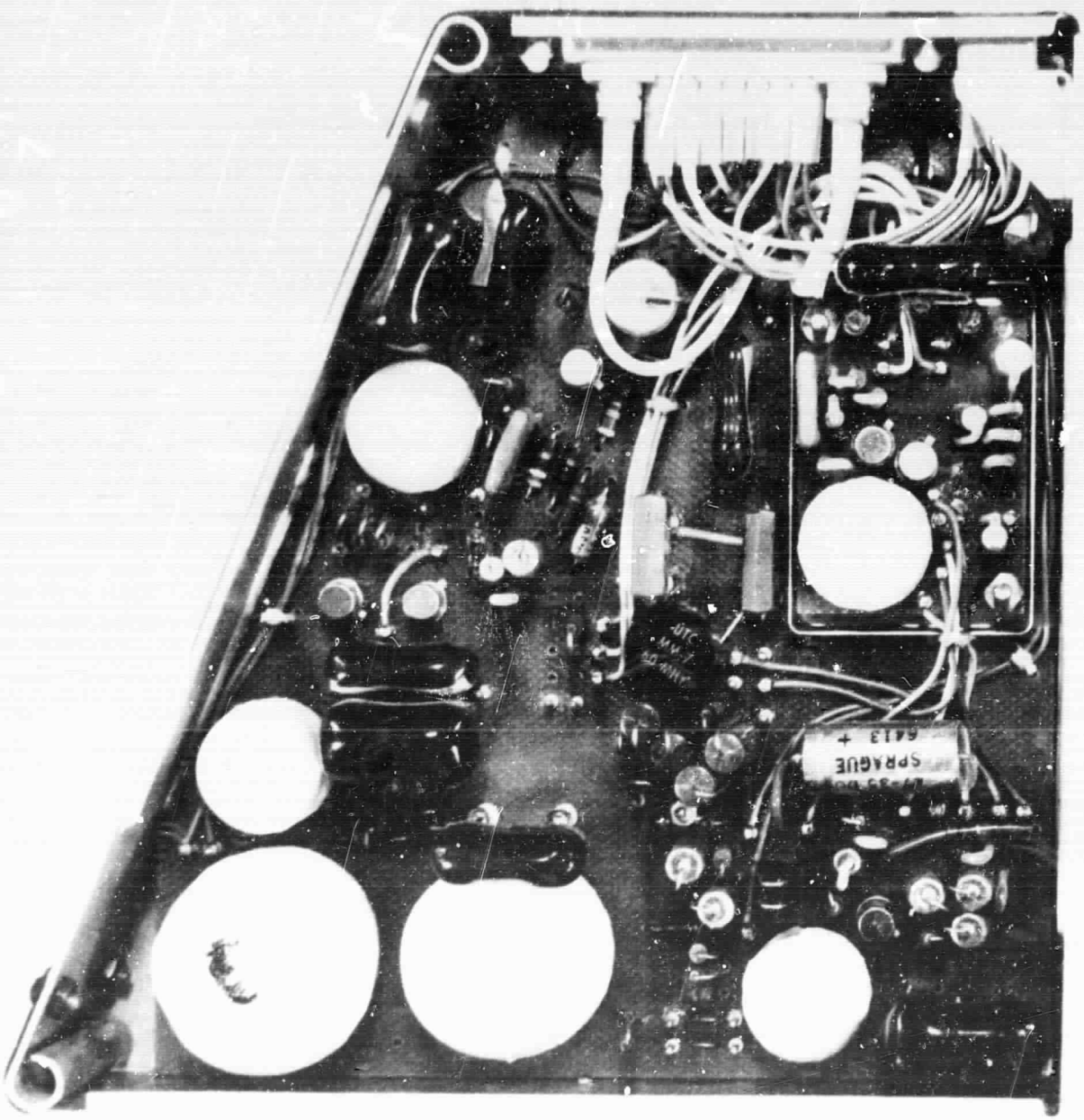

FIG. 11

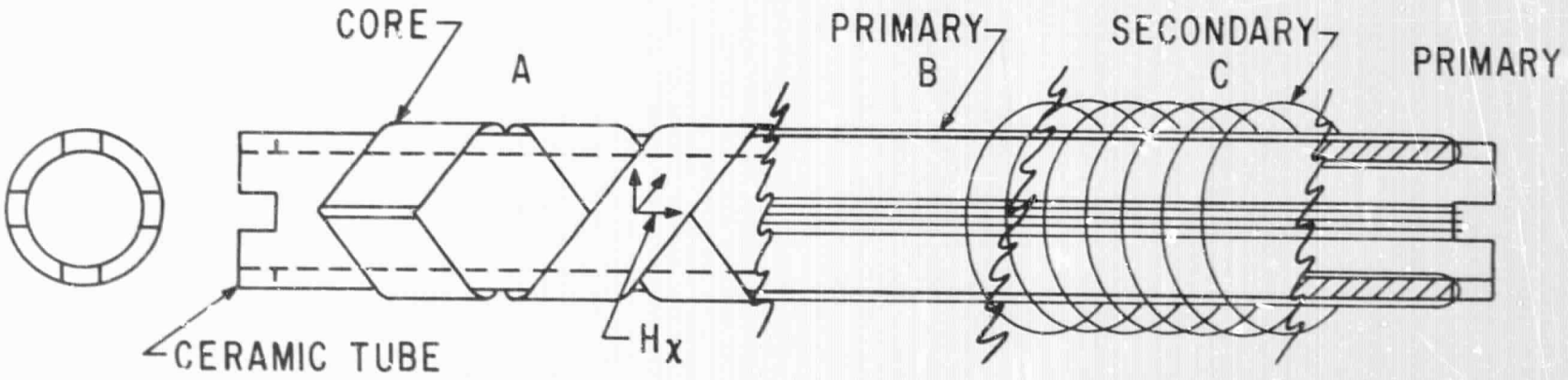

FLUXGATE SENSOR

FIG. 13

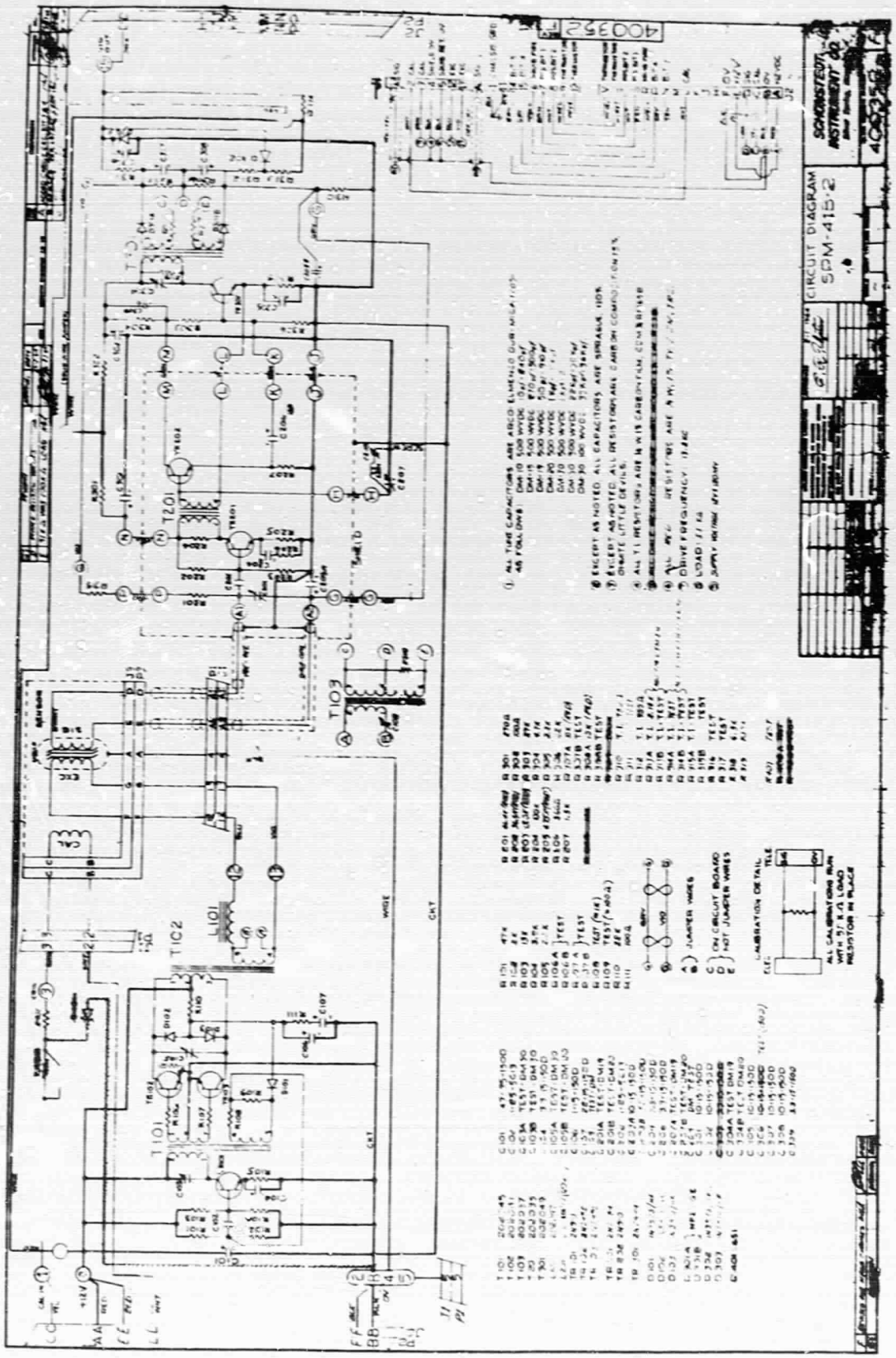

FIG. 14

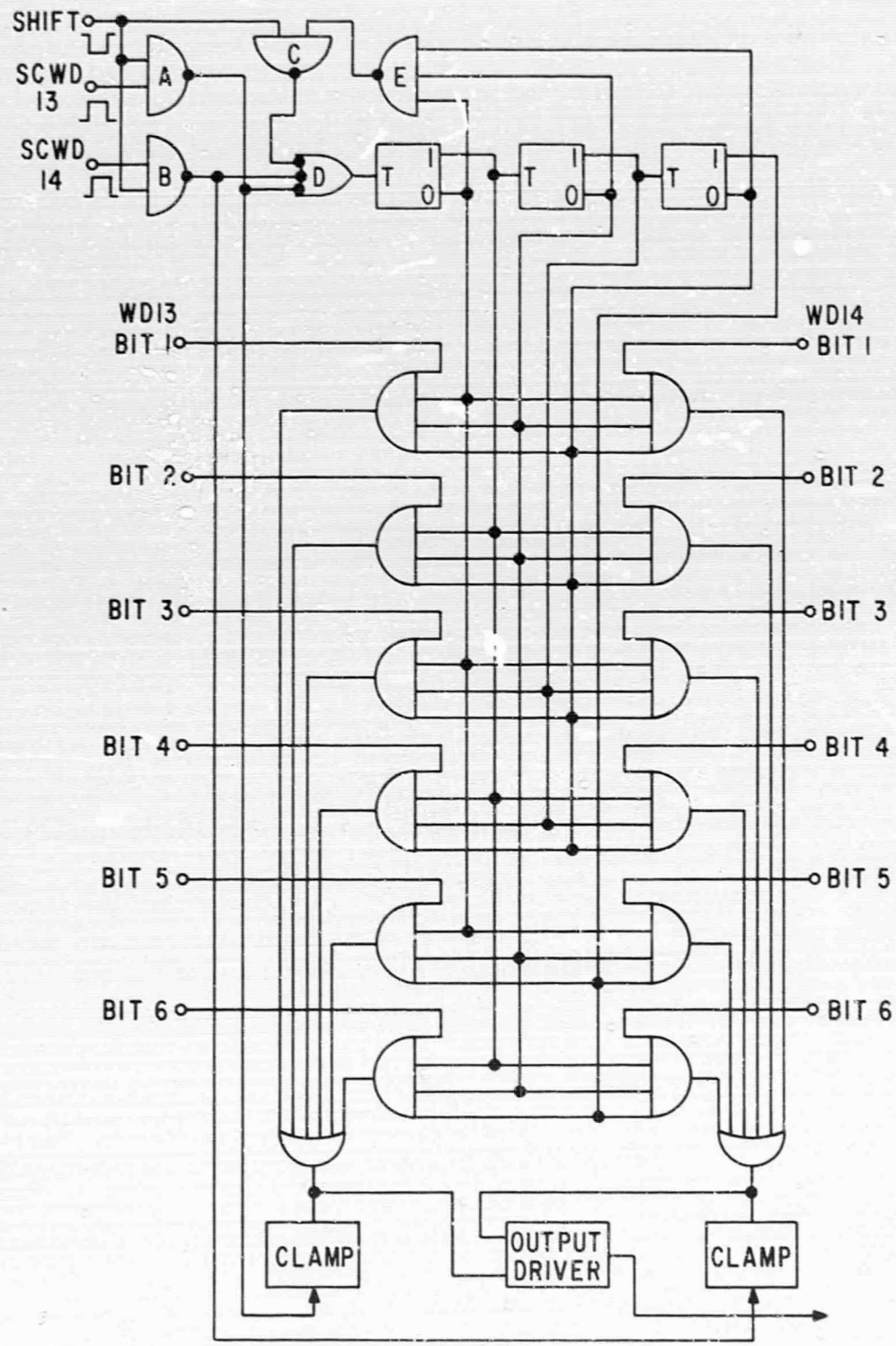

HOUSEKEEPING DATA SYSTEM

FIG. 15

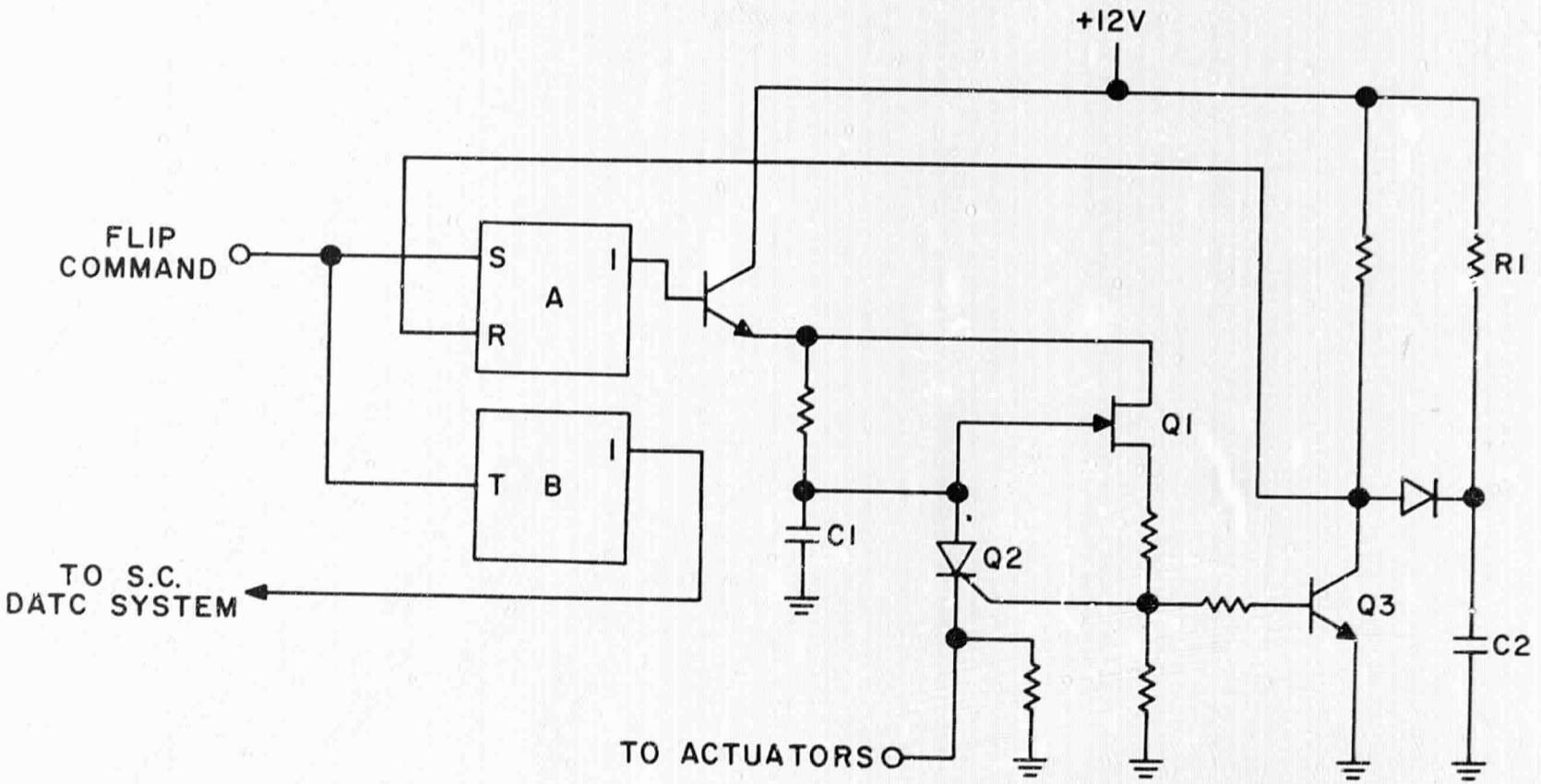
+12V
FLIP
COMMAND
S
I
A
R
T
B
I
R1
Q1
C1
Q2
Q3
C2
TO S.C.
DATC SYSTEM
TO ACTUATORS

FIG. 16

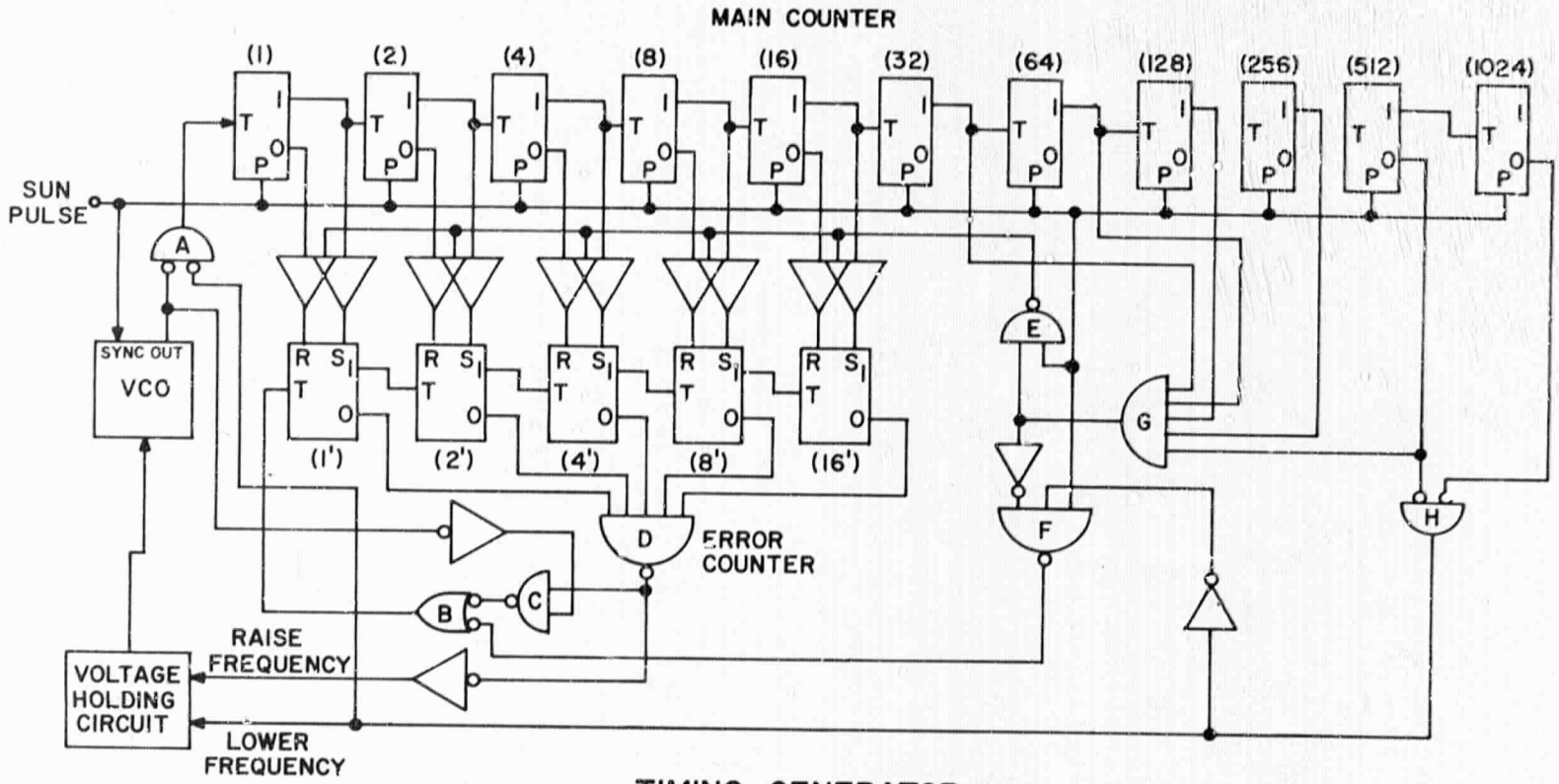

TIMING GENERATOR
FIG. 17

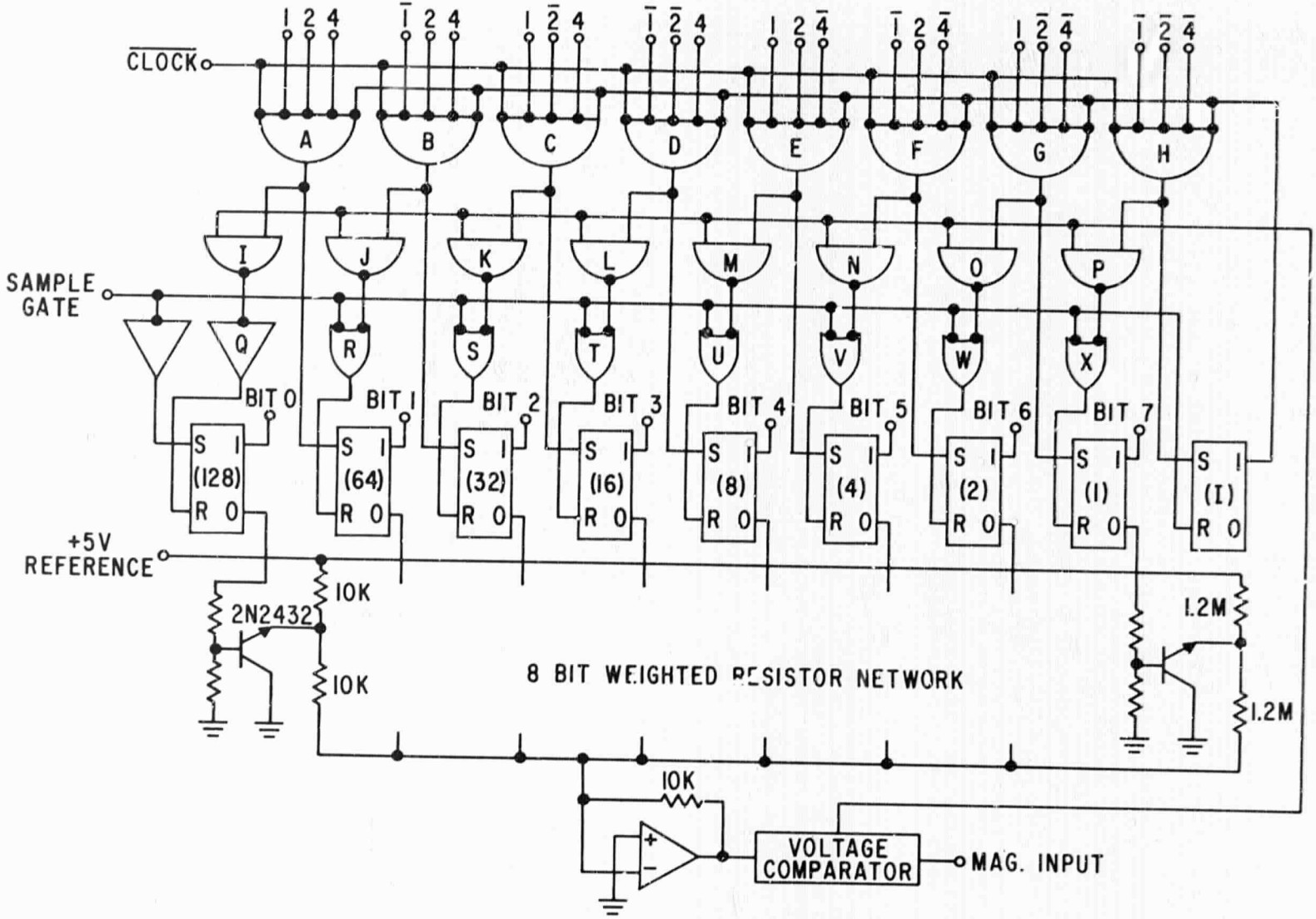

ANALOG TO DIGITAL CONVERTOR

FIG. 18

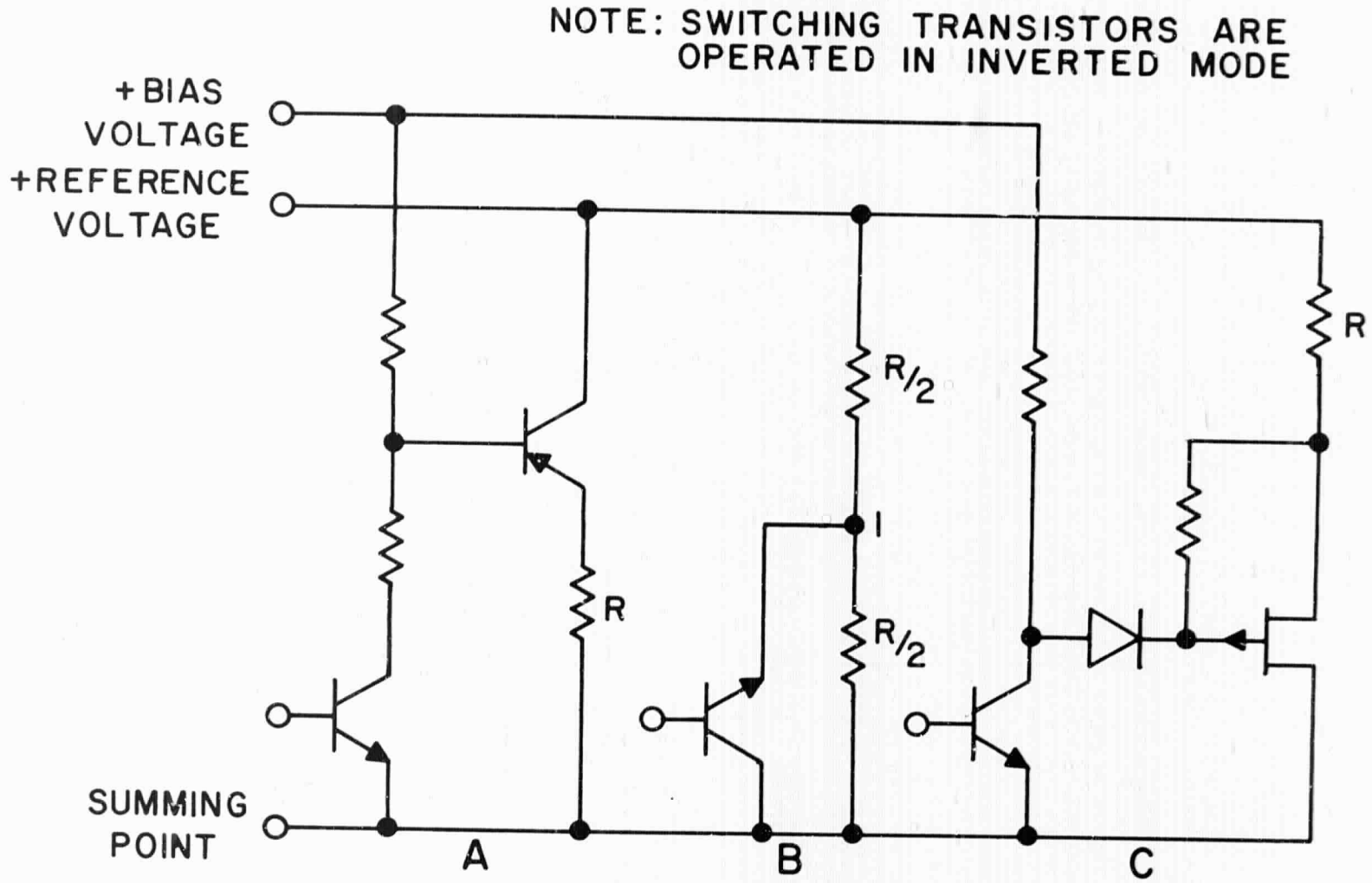

CURRENT SWITCHING CIRCUITS

FIG. 19

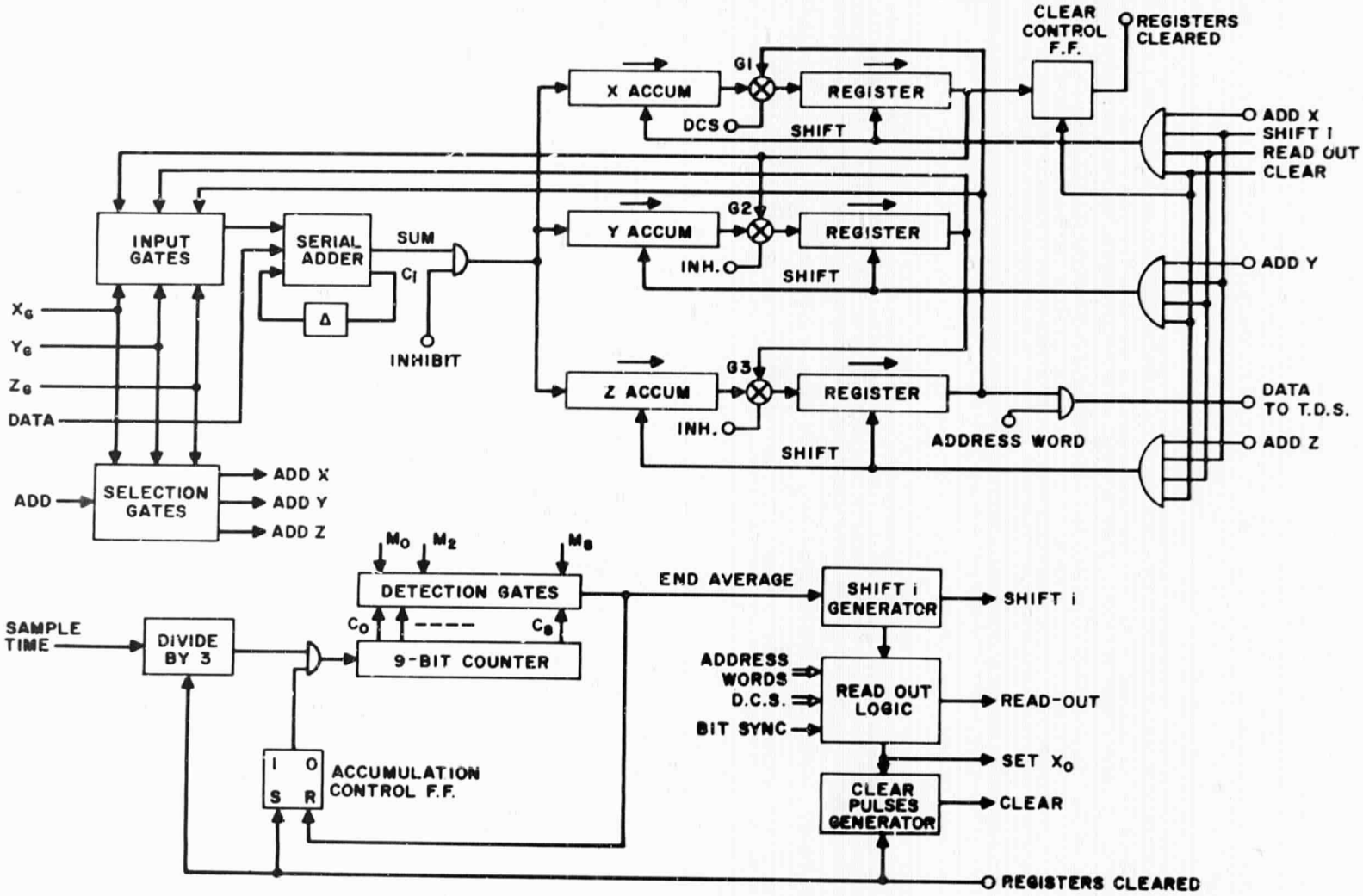

Figure 20. Time Average Unit Block Diagram

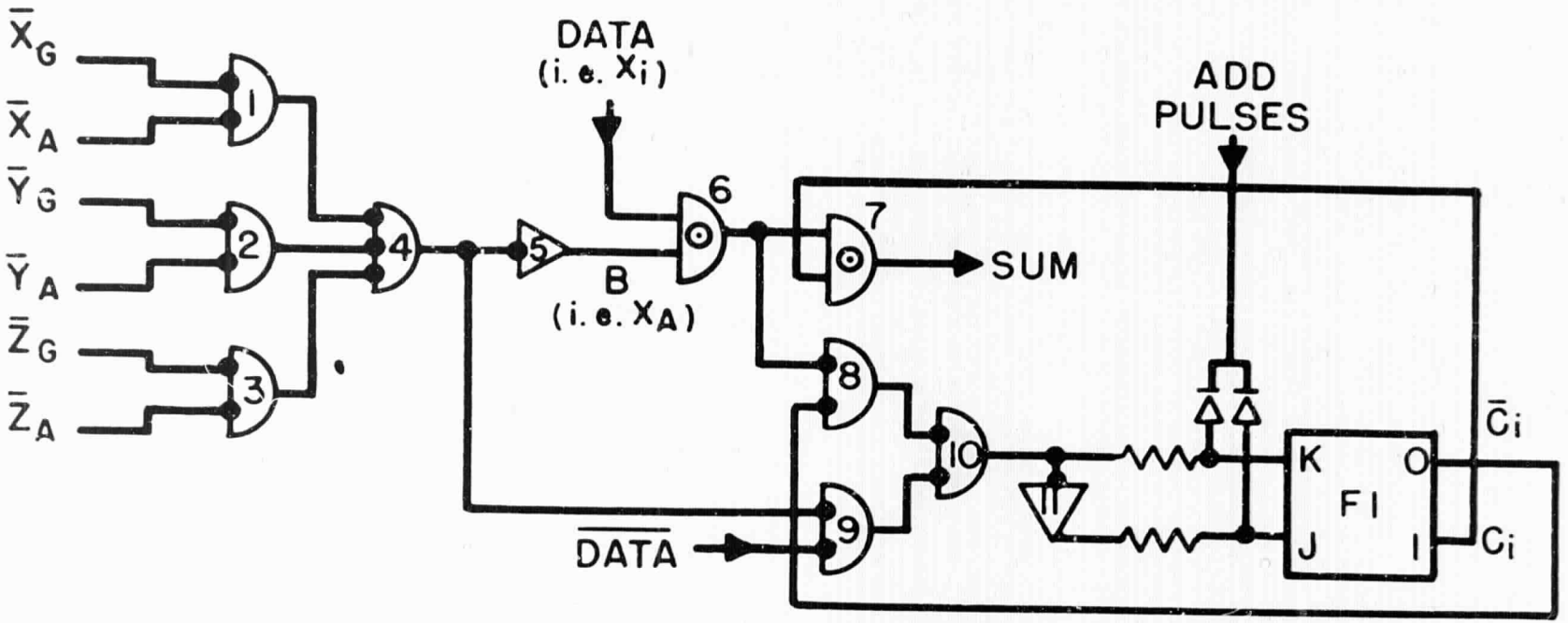

Figure 21. Serial Adder

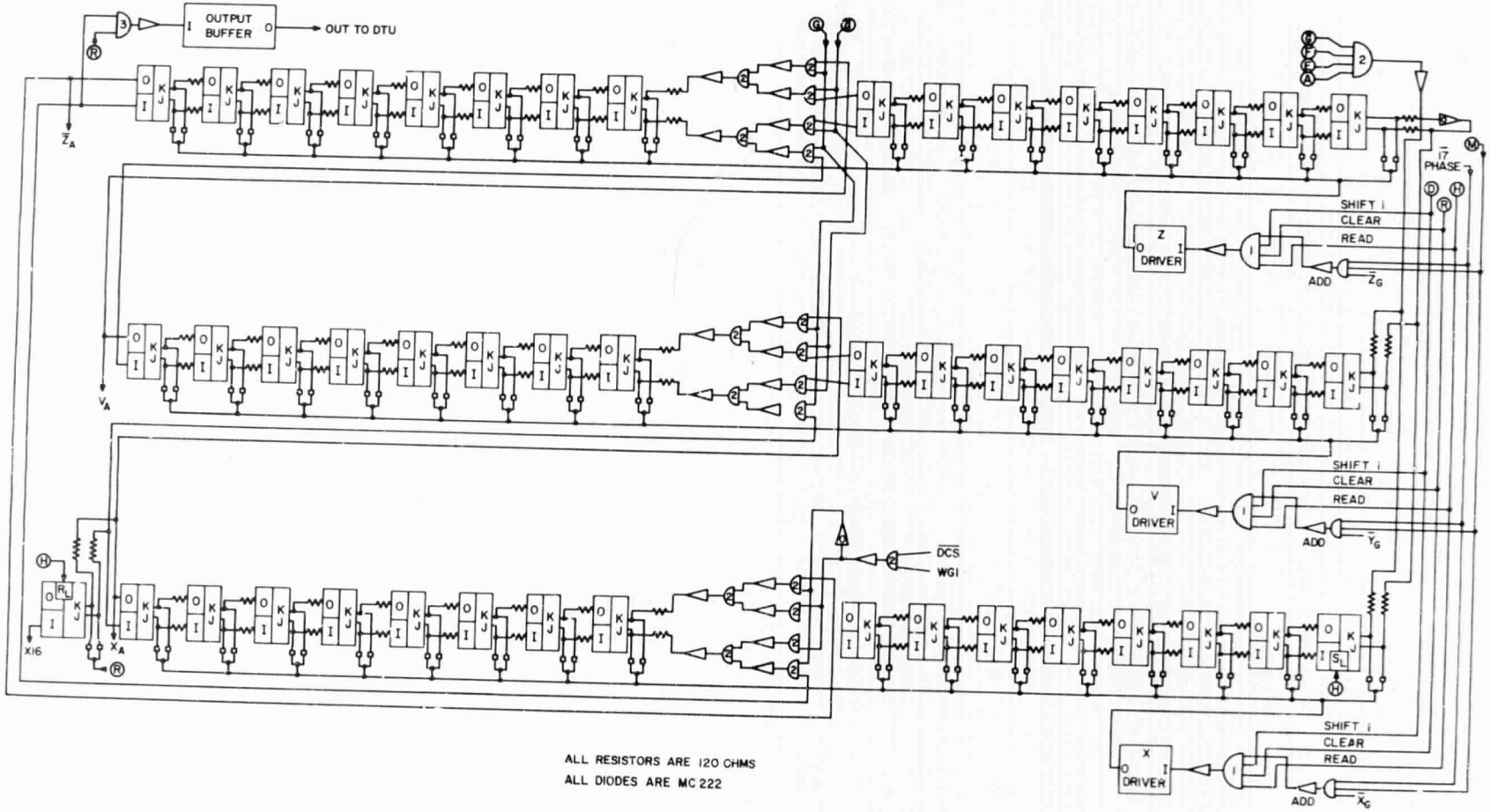

X,Y,Z ACCUMULATOR REGISTERS PIONEER TIME AVERAGE COMPUTER

FIG. 22

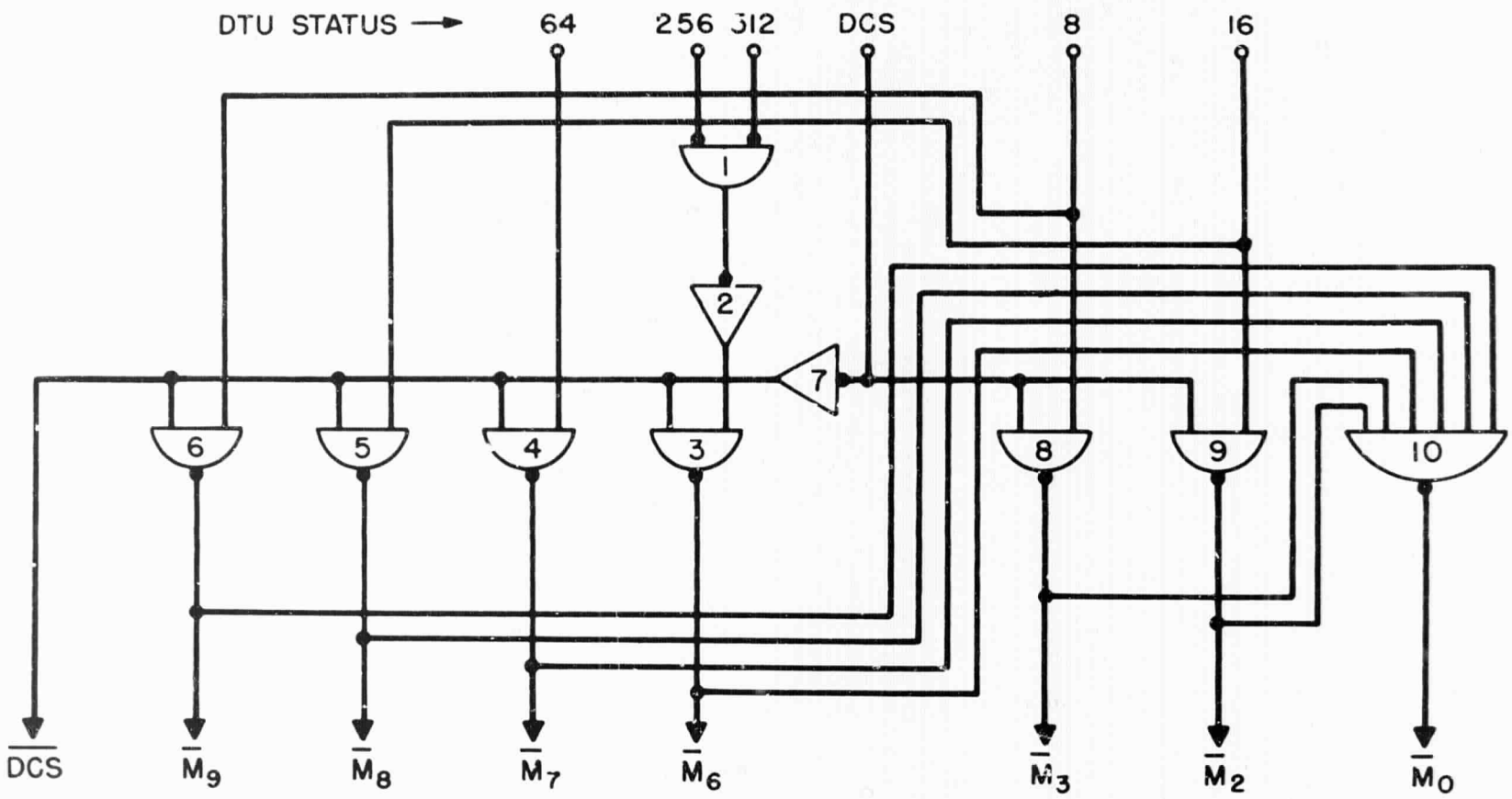

Figure 23. Averaging Mode Selector

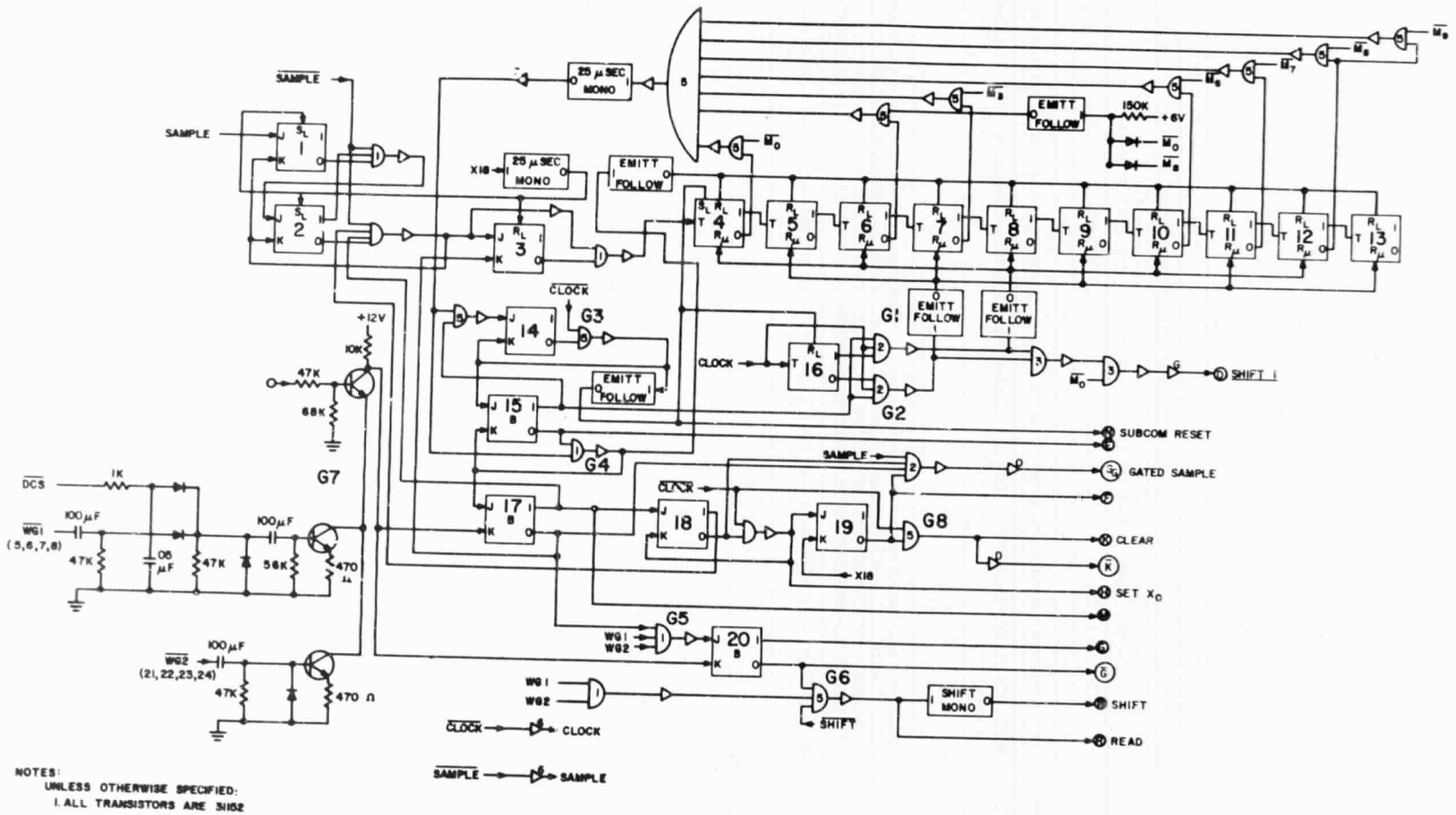

NOTES:
UNLESS OTHERWISE SPECIFIED:
1. ALL TRANSISTORS ARE 3N52

TIME AVERAGE COMPUTER PROGRAMMER

FIG. 24